ACS APPLIED POLYMER MATERIALS

pubs.acs.org/acsapm Article

Biotinylated RAFT Styrene/Maleic Acid Copolymers for Biosensor Applications of Membrane Proteins

Marco Antônio G. B. Gomes, David Glueck, Valentin Monjal, Marjorie Damian, Pierre Guillet, Jean-Louis Banères, Sandro Keller, and Grégory Durand*

Cite This: https://doi.org/10.1021/acsapm.5c02955 Read Online

ACCESS | Metrics & More | Article Recommendations | Supporting Information

ABSTRACT: We report the RAFT polymerization of biotinylated styrene/maleic anhydride (SMAnh) copolymers using a biotin-PEG$_n$-modified transfer agent. These polymers exhibit degrees of polymerization ranging from 32 to 45 and narrow molar mass distributions from 4000 to 7000 g mol^{-1}, with a dispersity ($Đ$) around 1.20. Hydrolysis of SMAnh yielded water-soluble styrene/maleic acid (SMA) copolymers, which formed micelles with diameters of 9−13 nm on average. 1:1 mixtures of biotinylated and nonbiotinylated SMA copolymers were found to solubilize vesicles made from fully saturated zwitterionic phospholipids to form lipid-bilayer nanodiscs. These polymer mixtures were further tested using proteoliposomes composed of unsaturated zwitterionic and anionic phospholipids containing 10 mol % cholesterol as well as melanocortin 2 receptor accessory protein 2 (MRAP2) or human ghrelin receptor (GHSR) as monotopic and polytopic transmembrane proteins, respectively. Mixtures of biotinylated and nonbiotinylated SMA were similarly efficient in solubilizing these proteoliposomes as SMA and superior to di-isobutylene maleic acid (DIBMA) copolymer. After solubilization, the resulting biotinylated nanodiscs were efficiently and specifically immobilized onto streptavidin-coated surfaces, as demonstrated by surface plasmon resonance (SPR) spectroscopy. Crucially, immobilizing nanodiscs using biotinylated SMA did not impair the pharmacology properties of GHSR. From a chemical viewpoint, our approach ensures homogeneous polymer end-chain functionalization, overcoming limitations associated with postpolymerization modification. From an application viewpoint, biotinylated SMA copolymers offer a robust and versatile platform for immobilizing membrane proteins within their native lipid environment for biosensing and ligand screening applications without the need to modify proteins directly.

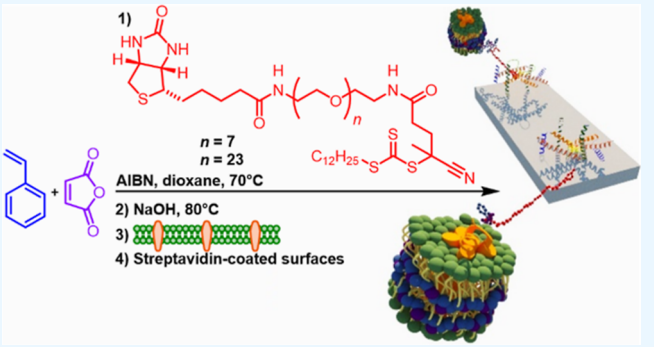

KEYWORDS: *RAFT polymerization, styrene−maleic acid copolymers, biotinylation, nanodiscs, membrane proteins, biosensors*

INTRODUCTION

Membrane proteins are the targets for nearly 60% of currently available drugs.[1] Although membrane proteins account for about 30% of the human proteome,[2] they represent only 3−4% of resolved structures in the Protein Data Bank (PDB).[1] This low percentage is attributed to the challenges associated with maintaining the native three-dimensional conformation of membrane proteins during extraction from lipid membranes, as well as challenges during downstream purification and characterization. Detergents are the most commonly used molecules for membrane solubilization and the subsequent extraction and purification of membrane proteins.[3] Over the past two decades, several chemically designed alternatives to classical detergents have been explored, including branched,[4] cyclic,[5] and fluorinated detergents[6,7] as well as neopentyl,[8] facial,[9,10] and calixarene derivatives,[11] to name but a few. Additionally, nondetergent heterogeneous systems such as bicelles,[12,13] as well as polymers, and nanodiscs have been extensively studied.[14−16]

In 2009, Knowles et al.[17] demonstrated that styrene/maleic acid (SMA) copolymers are able to directly solubilize membrane proteins into nanodiscs, disc-shaped nanostructures containing a lipid bilayer surrounded by a belt of polymer chains, also known as SMA lipid particles (SMALPs). SMA copolymers with a styrene/maleic acid ratios between 2:1 and 3:1 form nanodiscs ranging from 10 to 30 nm in diameter, providing a nanoscale lipid environment for membrane proteins.[18] Since then, research in this area has grown rapidly.[19−26] From a chemical viewpoint, SMA polymers were initially prepared by conventional free radical polymerization. More recently, reversible addition−fragmentation

Received: August 18, 2025
Revised: October 3, 2025
Accepted: October 6, 2025

chain transfer (RAFT) polymerization was used to produce well-defined polymers,[18] enhance monomer sequence control,[27,28] and introduce selected end groups via the chain transfer agent (CTA).[29,30] Synthetic routes for structural analogs of SMA have also been developed where the charge[31] or the hydrophobic balance[32] of the polymer can be varied. Another important modification is the replacement of the aromatic ring by an isobutylene group to form diisobutylene/maleic acid (DIBMA) copolymers.[33,34]

Membrane-protein immobilization onto surfaces or beads in their native state has gained increasing interest for facilitating purification and ligand screening. Functional immobilization can be achieved using engineered protein tags or modified surfaces incorporating native and reconstituted membrane fragments.[35] Biotin is often the tag of choice due to its strong interaction with avidin and streptavidin ($K_a \sim 10^{15}$ M^{-1} and $K_a \sim 10^{13}$ M^{-1}, respectively),[36,37] and several modified surfaces bearing avidin or streptavidin are commercially available. Functionalized polymers with affinity tags provide a versatile means for membrane-protein immobilization. Specifically, biotin functionality has been widely introduced in various transfer agents leading to well-defined biotinylated polymers.[38−42] Biotinylated amphipol polymers have successfully enabled attachment onto solid supports.[43−45] In contrast, the use of biotinylated SMA nanodiscs has remained underexplored.

Here, we report the synthesis of two functionalized transfer agents comprising a biotin tag attached to the reactive part of the transfer agent via a polyethylene glycol (PEG) spacer containing 7 or 23 PEG units. PEG spacers are widely used in bioconjugation strategies because they improve solubility, minimize steric hindrance, and provide conformational flexibility to functional groups.[46,47] In this work, the use of short PEG linkers was expected to improve the accessibility of the biotin moiety and facilitate efficient binding to streptavidin-coated surfaces. These transfer agents were used for the copolymerization of styrene and maleic anhydride via RAFT polymerization, yielding a series of well-defined biotinylated SMA polymers. To the best of our knowledge, this is the first time that short PEG spacers are introduced between the biotin functionality and a RAFT transfer agent bearing a trithiocarbonate functionality.

We characterized the lipid-solubilization efficiency of biotinylated SMA on large unilamellar vesicles (LUVs) composed of pure 1,2-dimyristoyl-*sn*-glycero-3-phosphocholine (DMPC). We also tested the potency of the biotinylated SMA to solubilize and keep functional two model membrane proteins with different structural organization, namely, the monotopic transmembrane protein melanocortin 2 receptor accessory protein 2 (MRAP2) and the polytopic human ghrelin receptor (GHSR), both embedded in liposomes composed of 9:1 (mol/mol) mixtures of the singly unsaturated phospholipids 1-palmitoyl-2-oleoyl-*sn*-glycero-3-phosphocholine (POPC) and 1-palmitoyl-2-oleoyl-*sn*-glycero-3-phosphoglycerol (POPG) with 10 mol % cholesterol. We demonstrated that the two model proteins GHSR and MRAP2 extracted into biotinylated nanodiscs can be immobilized onto streptavidin surfaces for surface plasmon resonance (SPR) spectroscopy. Finally, we showed that our polymers preserved the pharmacological properties of GHSR after attachment to a functionalized surface and that the immobilized receptor can be used for ligand screening.

EXPERIMENTAL SECTION

All common reagents were commercially available and purchased from Merck (Darmstadt, Germany) and TCI Europe N.V. (Zwijndrecht, Belgium). Biotin-PEG_7-NH_2 and biotin-PEG_{23}-NH_2 were obtained from Sirius Fine Chemicals—SiChem (Bremen, Germany) where, PEG_7 and PEG_{23} refer to the number of PEG units, corresponding to molecular weights of about 300 and 1000 Da, respectively. All solvents were of reagent grade and used as received. NMR spectra were recorded with a Bruker AC400 operating at 400 MHz for ^{1}H and 100 MHz for ^{13}C analyses; chemical shifts are given in ppm relative to the solvent residual. Analytical HPLC were performed using a Shimadzu system equipped with Waters XTerra RP18 column (100 × 2.1 mm, 5 μm), CBM-20A controller, DGU-20A3 degassing device, LC-20 AD solvent delivery system, and SPD-M20A photodiode detection. The mobile phase was 1%TFA in ACN × 1%TFA in milli-Q water ($t_{0\ min.}$ = 1:9, $t_{22\ min.}$ = 9.5:0.5, $t_{31\ min.}$ = 1:9), at a flow rate of 1.0 mL/min. Preparative HPLC were performed on a Waters 2487 system equipped with a Waters Sunfire C18 OBD column (19 × 250 mm, 5 μM) and detector 214 nm. Analytical SEC were performed using a Shimadzu system, equipped with two detectors: a Shimadzu RID-20A RI detector and a Shimadzu UV detector SPD-40. Separations were performed using a PSS guard column GRAM 10 μm 8 × 50 mm and two PSS column GRAM 100 Å 10 μm 8 × 300 mm. The mobile phase was a solution of 0.05 mol L^{-1} LiBr in DMF, at a flow rate of 0.5 mL/min at 40 °C. The calibration was established using polystyrene, (1050−19,000 kDa) from Polymer Laboratories Ltd. HRMS were performed using a Waters UPLC I-Class system coupled with a SynaptG2Si QTof MS (Waters, Milford, USA). Mobile phases were constituted of water with 0.1% formic acid (A) and acetonitrile with 0.1% formic acid (B). Data were acquired in positive ionization mode in high-resolution mode from 50 m/z to 1200 m/z with a scan time of 0.1 scan/s using MSe (low energy 4 eV and high-energy ramp from 25 to 50 eV). Commercial SMA used for the production of DMPC nanodiscs, *Escherichia coli* membrane solubilization, and SPR investigation was obtained from Polyscope. SMA(2:1) was hydrolyzed from SMAnh (Xiran SZ30010), and SMA(3:1) was hydrolyzed from Xiran SL25010, as detailed in Grethen et al.[48] Commercial SMA and DIBMA used for the solubilization of MRAP2 and GHSR were obtained from Cube Biotech.

Synthesis of CDTPA. (1). CDTPA, used as the RAFT agent, was synthesized using the methodology described by Lin et al.[49]

Synthesis of NHS-CDTPA. (2). Compound **2** was synthesized from an adapted protocol described by Wang et al.[38] In a round-flask containing dichloromethane (10.00 mL), were added at 0 °C, 4-cyano-4-[(dodecylsulfanylthiocarbonyl)sulfanyl]pentanoic acid (**1**), (1.00 g, 3.10 mmol, 1.00 equiv), *N*-hydroxysuccinimide (NHS) (0.36 g, 3.10 mmol, 1.00 equiv) and 1-ethyl-3-(3-(dimethylamino)-propyl)carbodiimide (EDC) (0.62 g, 3.23 mmol, 1.05 equiv). The reaction mixture was stirred for 2 h at 0 °C, then warmed to room temperature and stirred for another 16 h. The crude product was extracted into dichloromethane, and the organic layer was washed with a solution of sodium bicarbonate, dried with magnesium sulfate, and concentrated under reduced pressure to yield NHS-CDTPA (**2**) (1.20 g, 2.40 mmol, 96%) as a yellow solid without any purification. ^{1}H NMR (400 MHz, $CDCl_3$, 298 K) δ: 3.30 (t, 2H, J = 7.5 Hz, CH_2), 2.96−2.89 (m, 2H, CH_2), 2.84 (s, 4H, CH_2), 2.70−2.59 (m, 1H, CH_2), 2.56−2.47 (m, 1H, CH_2), 1.87 (s, 3H, CH_3), 1.69 (m, 2H, J = 7.3 Hz CH_2), 1.44−1.33 (m, 2H, CH_2), 1.25 (s, 16H, CH_2), 0.87 (t, 3H, J = 6.7 Hz, CH_3). ^{13}C NMR (100 MHz, $CDCl_3$, 298 K) δ: 216.6 (C), 168.9 (2 × C), 167.1 (C), 118.7 (C), 46.1 (CH_2), 37.2 (CH_2), 33.2 (CH_2), 32.0 (CH_2), 29.7 (2 × CH_2), 29.6 (CH_2), 29.5 (CH_2), 29.4 (CH_2), 29.1 (CH_2), 29.0 (CH_2), 27.7 (CH_2), 26.9 (CH_2), 25.6 (2 × CH_2), 24.8 (CH_2), 22.7 (CH_3), 14.2 (CH_3).

Synthesis of Biotin-PEG_7-CDTPA. (3a). In a round-flask with dimethylformamide (1.00 mL) were added biotin-PEG_7-NH_2 (0.20 g, 0.33 mmol, 1.00 equiv), NHS-CDTPA (**2**) (0.17 g, 0.33 mmol, 1.00 equiv) and triethylamine (TEA) (92 μL, 0.63 mmol, 1.90 equiv). The reaction mixture was stirred for 24 h and concentrated under reduced

https://doi.org/10.1021/acsapm.5c02955
ACS Appl. Polym. Mater. XXXX, XXX, XXX−XXX

pressure. The crude was solubilized in acetonitrile (10 mL), and the residual precipitate, identified as dodecane-1-thiol, was filtered off. The soluble part was purified by preparative HPLC, using a mixture of acetonitrile/water ranging from 0:100 to 95:5 (*v*/*v*). After removal of the solvents under reduced pressure, biotin-PEG$_7$-CDTPA (**3a**) (0.20 g, 0.20 mmol, 62%) was isolated as a yellow oil. ^{1}H NMR (400 MHz, $CDCl_3$, 298 K) δ: 6.90−6.74 (m, 2H, NH), 6.21 (s, 1H, NH), 4.51 (dd, 1H, J = 7.1 Hz, 5.2 Hz, CH), 4.32 (dd, 1H, J = 7.6 Hz, 4.6 Hz, CH), 3.66−3.59 (m, 21H, CH_2), 3.56 (t, 4H, J = 4.7 Hz, CH_2), 3.47−3.39 (m, 4H, CH_2), 3.31 (t, 2H, J = 7.4 Hz, CH_2), 3.21−3.09 (m, 1H, CH), 2.96−2.86 (m, 1H, CH_2), 2.57 (d, 1H, J = 13.0 Hz, CH_2), 2.56−2.45 (m, 3H, CH_2), 2.41−2.28 (m, 1H, CH_2), 2.23 (t, 2H, J = 7.4 Hz, CH_2), 1.88 (s, 3H, CH_3), 1.80−1.58 (m, 6H, CH_2), 1.49−1.33 (m, 4H, CH_2), 1.25 (s, 17H, CH_2), 0.87 (t, 3H, J = 6.7 Hz, CH_3). ^{13}C NMR (100 MHz, $CDCl_3$, 298 K) δ: 217.3 (C), 173.3 (C), 170.5 (2 × C), 119.3 (C), 70.4 (4 × CH_2), 70.4 (4 × CH_2), 70.4 (CH_2), 70.3 (CH_2), 70.1 (CH_2), 70.0 (CH_2), 69.8 (CH_2), 69.7 (CH_2), 61.8 (CH), 60.2 (CH), 55.4 (CH), 46.8 (CH_2), 40.4 (CH_2), 39.4 (CH_2), 39.1 (CH_2), 37.0 (C), 35.7 (CH_2), 34.5 (CH_2), 31.8 (CH_2), 31.4 (CH_2), 29.6 (2 × CH_2), 29.5 (CH_2), 29.4 (CH_2), 29.3 (CH_2), 29.0 (CH_2), 28.9 (CH_2), 28.0 (CH_2), 28.0 (CH_2), 27.6 (CH_2), 25.5 (CH_2), 28.8 (CH_2), 22.6 (CH_3), 14.1 (CH_3). Purity (HPLC, 214 nm): 96.08%. HRMS (ESI) *m*/*z*: $[M + H]^+$ calcd for $C_{45}H_{81}N_5O_{10}S_4$, 980.4945; found, 980.4958 and $[M + Na]^+$ calcd for $C_{45}H_{81}N_5O_{10}S_4$, 1002.4764; found, 1002.4772.

Synthesis of Biotin-PEG$_{23}$-CDTPA (3b). In a round-flask with *N*,*N*-dimethylformamide (1.00 mL) were added Biotin-PEG$_{23}$-NH_2 (0.20 g, 0.15 mmol, 1.00 equiv), NHS-CDTPA (**2**) (0.075 g, 0.15 mmol, 1.00 equiv) and triethylamine (TEA) (41 μL, 0.30 mmol, 2.00 equiv). The reaction mixture was stirred for 24 h and concentrated under reduced pressure. The crude was purified by gravity size-exclusion chromatography (Sephadex LH-20 resin, CH_2Cl_2/MeOH 1:1 *v*/*v*). After removal of the solvents, Biotin-PEG$_{23}$-CDTPA (**3b**) (0.22 g, 0.13 mmol, 86%) was obtained as a yellow oil. ^{1}H NMR (400 MHz, $CDCl_3$, 298 K) δ: 6.89 (s, 1H, NH), 6.72 (s, 1H, NH), 4.52 (dd, 1H, J = 6.7 Hz, 4.7 Hz, CH), 4.33 (dd, 1H, J = 7.5 Hz, 4.3 Hz, CH), 3.65−3.60 (m, 89H, CH_2), 3.55 (t, 4H, J = 5.1 Hz, CH_2), 3.45−3.40 (m, 4H, CH_2), 3.31 (t, 2H, J = 7.3 Hz, CH_2), 3.19−3.11 (m, 1H, CH), 2.94−2.86 (m, 1H, CH_2), 2.76 (d, 1H, J = 12.9 Hz, CH_2), 2.51−2.45 (m, 3H, CH_2), 2.36−2.32 (m, 1H, CH_2), 2.23 (t, 2H, J = 7.2 Hz, CH_2), 1.87 (s, 3H, CH_3), 1.76−1.59 (m, 6H, CH_2), 1.49−1.33 (m, 4H, CH_2), 1.24 (s, 17H, CH_2), 0.86 (t, 3H, J = 6.9 Hz, CH_3). ^{13}C NMR (100 MHz, $CDCl_3$, 298 K) δ: 217.3 (C), 173.3 (C), 170.5 (2 × C), 119.3 (C), 70.6 (41 × CH_2), 70.5 (CH_2), 70.5 (CH_2), 70.3 (CH_2), 70.2 (CH_2), 69.9 (CH_2), 69.7 (CH_2), 62.0 (CH), 60.5 (CH), 55.4 (CH), 46.8 (CH_2), 40.5 (CH_2), 39.5 (CH_2), 39.3 (CH_2), 37.1 (C), 35.7 (CH_2), 34.6 (CH_2), 32.0 (CH_2), 31.6 (CH_2), 29.7 (2 × CH_2), 29.6 (CH_2), 29.5 (CH_2), 29.4 (CH_2), 29.1 (CH_2), 29.0 (CH_2), 28.1 (CH_2), 27.8 (CH_2), 25.6 (CH_2), 25.0 (CH_2), 22.7 (CH_3), 14.2 (CH_3). Purity (HPLC, 214 nm): 97.75%. HRMS (ESI) *m*/*z*: $[M + H]^+$ calcd for $C_{77}H_{145}N_5O_{26}S_4$, 1684.9139; found, 1684.9083 and $[M + Na]^+$ calcd for $C_{77}H_{145}N_5O_{26}S_4$, 1706.8958; found, 1706.8901.

General Procedure to SMAnh (6−7) and Biotin-SMAnh Polymerization. (8−11). In a Schlenk tube with 1,4-dioxane (1.00 mL) were added styrene (**4**) and maleic anhydride (**5**) (3:1 or 2:1 molar ratio), CDTPA (**1**) or PEG$_n$-CDTPA (**3**) (1/45 molar ratio) and AIBN (0.2 eq. mol to (**1**) or (**3**)), and degassed by freeze−pump−thaw cycles (4×). The mixture was stirred for 16 h at 70 °C. The SMAnh was precipitated into isopropanol, followed by centrifugation, and the resulting polymers were dried under vacuum.

(3:1)-SMAnh (**6a**). From styrene (**4**) (0.24 mL, 2.13 mmol), maleic anhydride (**5**) (0.070 g, 0.71 mmol), CDTPA (**1**) (0.060 g, 0.062 mmol) and AIBN (2.00 mg, 0.012 mmol), **6a** (0.16 g) was obtained as a pale-yellow powder. ^{1}H NMR (400 MHz, DMSO-d_6, 298 K) δ: 7.67−5.46 (br, 143 H, $CH_{arom.}$), 3.76−3.35 (br, 5H, CH_2/CH), 3.30−2.51 (br, 25H, CH_2/CH), 2.48−1.07 (br, 105H, CH_2/CH), 0.84 (br, 3H, CH_3). SEC (PSS, 0.05 mol L^{-1} LiBr in DMF, RI and UV detection, PS calibration): M_n = 3392 g/mol; M_w = 4218 g/mol; $Đ$ = 1.24.

(3:1)-SMAnh (**6b**). From styrene (**4**) (0.46 mL, 3.99 mmol), maleic anhydride (**5**) (0.13 g, 1.33 mmol), CDTPA (**1**) (0.047 g, 0.12 mmol) and AIBN (4.00 mg, 0.023 mmol), **6b** (0.44 g) was obtained as a pale-yellow powder. ^{1}H NMR (400 MHz, DMSO-d_6, 298 K) δ: 7.99−5.62 (br, 135H, $CH_{arom.}$), 3.55−3.34 (br, 4H, CH_2/CH), 3.31−2.52 (br, 24H, CH_2/CH), 2.47−1.07 (br, 100H, CH_2/CH), 0.84 (br, 3H, CH_3). SEC (PSS, 0.05 mol L^{-1} LiBr in DMF, RI and UV detection, PS calibration): M_n = 3448 g/mol, M_w = 4198 g/mol, $Đ$ = 1.21.

(2:1)-SMAnh (**7a**). From styrene (**4**) (0.41 mL, 3.54 mmol), maleic anhydride (**5**) (0.17 g, 1.77 mmol), CDTPA (**1**) (0.047 g, 0.12 mmol) and AIBN (4.00 mg, 0.023 mmol), **7a** (0.44 g) was obtained as a pale-yellow powder. ^{1}H NMR (400 MHz, DMSO-d_6, 298 K) δ: 7.59−5.69 (br, 134H, $CH_{arom.}$), 3.55−3.32 (br, 7H, CH_2/CH), 3.31−2.55 (br, 32H, CH_2/CH), 2.45−1.07 (br, 95H, CH_2/CH), 0.84 (br, 3H, CH_3). SEC (PSS, 0.05 mol L^{-1} LiBr in DMF, RI and UV detection, PS calibration): M_n = 3311 g/mol; M_w = 4001 g/mol; $Đ$ = 1.20.

(2:1)-SMAnh (**7b**). From styrene (**4**) (0.41 mL, 3.54 mmol), maleic anhydride (**5**) (0.17 g, 1.77 mmol), CDTPA (**1**) (0.047 g, 0.12 mmol) and AIBN (4.00 mg, 0.023 mmol), **7b** (0.37 g) was obtained as a pale-yellow powder. ^{1}H NMR (400 MHz, DMSO-d_6, 298 K) δ: 7.55−5.82 (br, 147H, $CH_{arom.}$), 3.54−3.32 (br, 8H, CH_2/CH), 3.31−2.57 (br, 38H, CH_2/CH), 2.43−1.15 (br, 96H, CH_2/CH), 0.84 (br, 3H, CH_3). SEC (PSS, 0.05 mol L^{-1} LiBr in DMF, RI and UV detection, PS calibration): M_n = 2940 g/mol; M_w = 3787 g/mol; $Đ$ = 1.28.

Biotin-PEG$_7$-(3:1)-SMAnh (**8a**). From styrene (**4**) (0.24 mL, 2.13 mmol), maleic anhydride (**5**) (0.070 g, 0.71 mmol), biotin-PEG$_7$-CDTPA (**3a**) (0.060 g, 0.062 mmol) and AIBN (2.00 mg, 0.012 mmol), **8a** (0.23 g) was obtained as a pale-yellow powder. ^{1}H NMR (400 MHz, DMSO-d_6, 298 K) δ: 7.53−5.70 (br, 138H, CH_{arom}), 4.30 (s, 1H, CH), 4.12 (s, 1H, CH), 3.50−3.32 (br, 30H, CH_2/CH), 3.31−2.51 (br, 34H, CH_2/CH), 2.48−1.07 (br, 108H, CH_2/CH), 0.84 (br, 3H, CH_3). SEC (PSS, 0.05 mol L^{-1} LiBr in DMF, RI and UV detection, PS calibration): M_n = 6293 g/mol; M_w = 7105 g/mol; $Đ$ = 1.12.

Biotin-PEG$_7$-(3:1)-SMAnh (**8b**). From styrene (**4**) (0.46 mL, 3.99 mmol), maleic anhydride (**5**) (0.13 g, 1.33 mmol), Biotin-PEG$_7$-CDTPA (**3a**) (0.11 g, 0.12 mmol) and AIBN (4.00 mg, 0.023 mmol), **8b** (0.44 g) was obtained as a pale-yellow powder. ^{1}H NMR (400 MHz, DMSO-d_6, 298 K) δ: 7.72−5.59 (br, 136H, $CH_{arom.}$), 4.29 (s, 1H, CH), 4.12 (s, 1H, CH), 3.56−3.33 (br, 29H, CH_2/CH), 3.32−2.51 (br, 32H, CH_2/CH), 2.48−1.06 (br, 108H, CH_2/CH), 0.84 (br, 3H, CH_3). SEC (PSS, 0.05 mol L^{-1} LiBr in DMF, RI and UV detection, PS calibration): M_n = 5785 g/mol; M_w = 6747 g/mol; $Đ$ = 1.16.

Biotin-PEG$_7$-(2:1)-SMAnh (**9a**). From styrene (**4**) (0.41 mL, 3.54 mmol), maleic anhydride (**5**) (0.17 g, 1.77 mmol), Biotin-PEG$_7$-CDTPA (**3a**) (0.11 g, 0.12 mmol) and AIBN (4.00 mg, 0.023 mmol), **9a** (0.32 g) was obtained as a pale-yellow powder. ^{1}H NMR (400 MHz, DMSO-d_6, 298 K) δ: 7.63−5.83 (br, 107H, $CH_{arom.}$), 4.26 (s, 1H, CH), 4.14 (s, 1H, CH), 3.65−3.33 (br, 34H, CH_2/CH), 3.32−2.52 (br, 41H, CH_2/CH), 2.47−1.13 (br, 83H, CH_2/CH), 0.84 (br, 3H, CH_3). SEC (PSS, 0.05 mol L^{-1} LiBr in DMF, RI and UV detection, PS calibration): M_n = 2829 g/mol; M_w = 3882 g/mol; $Đ$ = 1.37.

Biotin-PEG$_7$-(2:1)-SMAnh (**9b**). From styrene (**4**) (0.41 mL, 3.54 mmol), maleic anhydride (**5**) (0.17 g, 1.77 mmol), Biotin-PEG$_7$-CDTPA (**3a**) (0.11 g, 0.12 mmol) and AIBN (4.00 mg, 0.023 mmol), **9b** (0.27 g) was obtained as a pale-yellow powder. ^{1}H NMR (400 MHz, DMSO-d_6, 298 K) δ: 7.55−5.66 (br, 150H, $CH_{arom.}$), 4.29 (s, 1H, CH), 4.13 (s, 1H, CH), 3.52−3.33 (br, 36H, CH_2/CH), 3.31−2.54 (br, 39H, CH_2/CH), 2.45−1.15 (br, 116H, CH_2/CH), 0.84 (br, 3H, CH_3). SEC (PSS, 0.05 mol L^{-1} LiBr in DMF, RI and UV detection, PS calibration): M_n = 3775 g/mol; M_w = 5139 g/mol; $Đ$ = 1.36.

Biotin-PEG$_{23}$-(3:1)-SMAnh (**10**). From styrene (**4**) (0.39 mL, 3.37 mmol), maleic anhydride (**5**) (0.11 g, 1.12 mmol), Biotin-PEG$_{23}$-CDTPA (**3b**) (0.18 g, 0.10 mmol) and AIBN (4.00 mg, 0.023 mmol),

https://doi.org/10.1021/acsapm.5c02955
ACS Appl. Polym. Mater. XXXX, XXX, XXX−XXX

10 (0.39 g) was obtained as a pale-yellow powder. ^{1}H NMR (400 MHz, DMSO-d_6, 298 K) δ: 7.63−5.69 (br, 118H, $CH_{arom.}$), 4.29 (s, 1H, CH), 4.12 (s, 1H, CH), 3.58−3.33 (br, 100H, CH_2/CH), 3.32−2.54 (br, 35H, CH_2/CH), 2.45−1.09 (br, 90H, CH_2/CH), 0.84 (br, 3H, CH_3). SEC (PSS, 0.05 mol L^{-1} LiBr in DMF, RI and UV detection, PS calibration): M_n = 4582 g/mol; M_w = 5172 g/mol; $Đ$ = 1.12.

Biotin-PEG_{23}-(2:1)-SMAnh. (**11a**) From styrene (**4**) (0.35 mL, 3.00 mmol), maleic anhydride (**5**) (0.15 g, 1.50 mmol), Biotin-PEG_{23}-CDTPA (**3b**) (0.18 g, 0.10 mmol) and AIBN (4.00 mg, 0.023 mmol), **11a** (0.50 g) was obtained as a pale-yellow powder. ^{1}H NMR (400 MHz, DMSO-d_6, 298 K) δ: 7.57−5.70 (br, 119H, $CH_{arom.}$), 4.30 (s, 1H, CH), 4.12 (s, 1H, CH), 3.55−3.33 (br, 101H, CH_2/CH), 3.32−2.55 (br, 38H, CH_2/CH), 2.46−1.17 (br, 89H, CH_2/CH), 0.84 (br, 3H, CH_3). SEC (PSS, 0.05 mol L^{-1} LiBr in DMF, RI and UV detection, PS calibration): M_n = 5064 g/mol; M_w = 5839 g/mol; $Đ$ = 1.15.

Biotin-PEG_{23}-(2:1)-SMAnh. (**11b**) From styrene (**4**) (0.70 mL, 6.00 mmol), maleic anhydride (**5**) (0.30 g, 3.00 mmol), Biotin-PEG_{23}-CDTPA (**3b**) (0.34 g, 0.20 mmol) and AIBN (8.00 mg, 0.046 mmol), **11b** (0.90 g) was obtained as a pale-yellow powder. ^{1}H NMR (400 MHz, DMSO-d_6, 298 K) δ: 7.55−5.80 (br, 134H, $CH_{arom.}$), 4.30 (s, 1H, CH), 4.12 (s, 1H, CH), 3.54−3.33 (br, 106H, CH_2/CH), 3.32−2.53 (br, 40H, CH_2/CH), 2.46−1.18 (br, 100H, CH_2/CH), 0.84 (br, 3H, CH_3). SEC (PSS, 0.05 mol L^{-1} LiBr in DMF, RI and UV detection, PS calibration): M_n = 4589 g/mol; M_w = 5294 g/mol; $Đ$ = 1.15.

General Procedure to SMAnh and Biotin-SMAnh Hydrolysis (12−17). In a sealed tube with 1.0 M sodium hydroxide solution (2.00 mL) was added SMAnh (**6**−**7**) or biotin-SMAnh (**8**−**11**). The mixture was stirred for 4 h and dialyzed against water through 1 kDa molecular weight cutoff membranes, then the solvent was removed by lyophilization.

(3:1)-SMA (**12a**). From **6a** (0.11 g), **12a** (0.10 g) was obtained as a white powder. ^{1}H NMR (400 MHz, DMSO-d_6, 298 K) δ: 7.62−5.66 (br, 144H, CH_{arom}), 3.09−2.57 (br, 16H, CH_2/CH), 2.41−0.90 (br, 117H, CH_2/CH), 0.84 (br, 3H, CH_3).

(3:1)-SMA (**12b**). From **6b** (0.35 g), **12b** (0.38 g) was obtained as a white powder. ^{1}H NMR (400 MHz, DMSO-d_6, 298 K) δ: 7.81−5.76 (br, 135H, CH_{arom}), 3.19−2.57 (br, 13H, CH_2/CH), 2.44−0.89 (br, 114H, CH_2/CH), 0.84 (br, 3H, CH_3).

(2:1)-SMA (**13a**). From of **7a** (0.28 g), **13a** (0.28 g) was obtained as a white powder. ^{1}H NMR (400 MHz, DMSO-d_6, 298 K) δ: 8.04−5.80 (br, 125H, CH_{arom}), 3.26−2.75 (br, 23H, CH_2/CH), 2.37−1.00 (br, 104H, CH_2/CH), 0.84 (br, 3H, CH_3).

(2:1)-SMA (**13b**). From **7b** (0.22 g), **13b** (0.17 g) was obtained as a white powder. ^{1}H NMR (400 MHz, DMSO-d_6, 298 K) δ: 7.82−5.49 (br, 146H, CH_{arom}), 3.23−2.63 (br, 21H, CH_2/CH), 2.37−0.88 (br, 121H, CH_2/CH), 0.84 (br, 3H, CH_3).

Biotin-PEG_7-(3:1)-SMA (**14a**). From **8a** (0.17 g), **14a** (0.16 g) was obtained as a white powder. ^{1}H NMR (400 MHz, DMSO-d_6, 298 K) δ: 7.64−5.82 (br, 138H, CH_{arom}), 4.31 (s, 1H, CH), 4.13 (s, 1H, CH), 3.51−3.36 (br, 26H, CH_2), 3.24−2.55 (br, 28H, CH_2/CH), 2.46−0.89 (br, 118H, CH_2/CH), 0.84 (br, 3H, CH_3).

Biotin-PEG_7-(3:1)-SMA (**14b**). From **8b** (0.35 g), **14b** (0.34 g) was obtained as a white powder. ^{1}H NMR (400 MHz, DMSO-d_6, 298 K) δ: 7.72−5.58 (br, 130H, CH_{arom}), 4.29 (s, 1H, CH), 4.06 (s, 1H, CH), 3.50−3.42 (br, 27H, CH_2), 3.27−2.55 (br, 24H, CH_2/CH), 2.45−0.88 (br, 114H, CH_2/CH), 0.84 (br, 3H, CH_3).

Biotin-PEG_7-(2:1)-SMA (**15a**). From **9a** (0.28 g), **15a** (0.22 g) was obtained as a white powder. ^{1}H NMR (400 MHz, DMSO-d_6, 298 K) δ: 7.64−5.62 (br, 106H, CH_{arom}), 4.30 (s, 1H, CH), 4.11 (s, 1H, CH), 3.80−3.41 (br, 30H, CH_2), 3.29−2.57 (br, 31H, CH_2/CH), 2.45−0.91 (br, 95H, CH_2/CH), 0.84 (br, 3H, CH_3).

Biotin-PEG_7-(2:1)-SMA (**15b**). From **9b** (0.22 g), **15b** (0.14 g) was obtained as a white powder. ^{1}H NMR (400 MHz, DMSO-d_6, 298 K) δ: 7.65−5.57 (br, 147H, CH_{arom}), 4.30 (s, 1H, CH), 4.12 (s, 1H, CH), 3.74−3.43 (br, 30H, CH_2), 3.26−2.52 (br, 32H, CH_2/CH), 2.47−0.88 (br, 131H, CH_2/CH), 0.84 (br, 3H, CH_3).

Biotin-PEG_{23}-(3:1)-SMA (**16**). From **10** (0.37 g), **16** (0.36 g) was obtained as a white powder. ^{1}H NMR (400 MHz, DMSO-d_6, 298 K) δ: 7.69−5.79 (br, 118H, CH_{arom}), 4.30 (s, 1H, CH), 4.13 (s, 1H, CH), 3.71−3.44 (br, 93H, CH_2), 3.28−2.55 (br, 28H, CH_2/CH), 2.45−0.89 (br, 104H, CH_2/CH), 0.84 (br, 3H, CH_3).

Biotin-PEG_{23}-(2:1)-SMA (**17a**). From **11a** (0.48 g), **17a** (0.49 g) was obtained as a white powder. ^{1}H NMR (400 MHz, DMSO-d_6, 298 K) δ: 7.87−5.89 (br, 119H, CH_{arom}), 4.29 (s, 1H, CH), 4.13 (s, 1H, CH), 3.66−3.41 (br, 91H, CH_2), 3.28−2.55 (br, 27H, CH_2/CH), 2.45−0.90 (br, 111H, CH_2/CH), 0.84 (br, 3H, CH_3).

Biotin-PEG_{23}-(2:1)-SMA (**17b**). From **11b** (0.88 g), **17b** (0.81 g) was obtained as a white powder. ^{1}H NMR (400 MHz, DMSO-d_6, 298 K) δ: 7.70−5.76 (br, 130H, CH_{arom}), 4.29 (s, 1H, CH), 4.13 (s, 1H, CH), 3.61−3.42 (br, 99H, CH_2), 3.27−2.55 (br, 32H, CH_2/CH), 2.44−0.90 (br, 111H, CH_2/CH), 0.84 (br, 3H, CH_3).

Average Chemical Composition Determination. The average copolymer chemical composition (styrene molar fraction, F_S) was determined via ^{1}H NMR using the following equation (adapted from the literature)[50]

$$F_S = \frac{I_{aromatic} \times 0.2}{I^*_{aliphatic} \times 0.5 - I_{aromatic} \times 0.1}$$

with $I_{aromatic}$ corresponding to the integrated area under the five aromatic proton peaks at 5.90−8.00 ppm, $I^*_{aliphatic}$ the aliphatic protons at 0.90−3.80 ppm minus the contribution of CTA protons as illustrated in the equation below

$$I^*_{aliphatic} = I_{aliphatic} - I_{CTA}$$

with $I_{aliphatic}$ corresponding to the integrated total area under all aliphatic proton peaks (three from styrene and two from anhydride maleic/maleic acid) at 0.90−3.00 ppm and I_{CTA} the contribution of different CTA protons (29 for CDTPA; 72 for biotin-PEG_7-CDTPA, and 136 for biotin-PEG_{23}-CDTPA). The methyl group of CDTPA (δ 0.80−0.90) was first integrated and set to a value of 3. The aromatic and aliphatic region were then integrated relative to this.

Hydrodynamic Particle Size Distribution of Polymers. Size distribution of polymers was recorded on a Nano-S model 1600 (Malvern Instruments) equipped with a He−Ne laser (λ = 633 nm, 4.0 mW). The time-dependent correlation function of the scattered light intensity was measured at a fixed angle of 173° (backscattering detection). Measurements were performed using a 45 μL low-volume quartz batch cuvette (Hellma, Müllheim, Germany) at (25 ± 0.5) °C. Solutions of SMA (**12**−**13**) or biotin-SMA (**14**−**17**) at 50 mg/mL in PBS (pH 7.4) were prepared and filtered (0.45 μm) before being transferred to the cuvette.

Production of Nanodiscs. To prepare the lipids for non-fluorescent nanodiscs, dry DMPC powder was resuspended in PBS buffer (137 mM NaCl, 2.7 mM KCl, 10 mM Na_2HPO_4, 1.8 mM KH_2PO_4) via shaking for 3 h at 35 °C and 1000 rpm on a ThermoMixer (Eppendorf, Hamburg, Germany). Fluorescently labeled lipid vesicles were produced by dissolving DMPC and the fluorescent lipid Atto 488 PE in chloroform, followed by combination of the chloroform stocks to a DMPC/Atto 488 PE molar ratio of 99:5/0.5. Chloroform was evaporated under filtered N_2 gas, and chloroform traces were removed by storing the lipids under high vacuum overnight. Then, the lipid film was resuspended in PBS buffer. All lipid resuspensions were extruded in a Mini Extruder (Avanti Polar Lipids, Alabaster, USA) at 35 °C. Extrusion was performed with at least 13 repeats through two stacked polycarbonate membranes with a pore diameter of 100 nm (Cytiva, Freiburg, Germany). To produce nanodiscs, polymers were combined with the lipid films at the mass ratios noted in the results sections and a final lipid concentration of 5 mM. Samples were incubated overnight on a ThermoMixer at 800 rpm and 35 °C. Nanodisc size distributions were determined on a Nano Zetasizer μV (Malvern Instruments, Malvern, UK) equipped with an 830 nm laser and a detection angle of 90°. Measurements were performed at 35 °C with a 120 s equilibration time. Each sample was measured with the software-optimized attenuator position including 12 runs of 10 s per run.

https://doi.org/10.1021/acsapm.5c02955
ACS Appl. Polym. Mater. XXXX, XXX, XXX−XXX

Surface Plasmon Resonance Spectroscopy. SPR was carried out on a Biacore X100 instrument equipped with a CAP chip (both Cytiva, Austria). To immobilize nanodiscs, the chip was preconditioned by two 60 s injections of regeneration solution (6 M guanidine-HCl, 1 M NaOH), followed by immobilization of ssDNA−streptavidin as supplied with the CAPture reagent kit (Cytiva, Austria) according to the manufacturer's instructions. Then, the chip was equilibrated by consecutive 540 s PBS buffer (pH 7.4) and 0.1 mg/mL SMA(2:1), followed by a 540 s injection of the nanodisc sample for initial binding screens and 420 s for the analysis of concentration series. Immobilization stability was observed for 1200 s, followed by a 180 s injection of 1 mM SDS and 60 s of regeneration solution before the next injection cycle. All steps were carried out in PBS buffer, pH 7.4 at a flow of 10 μL/min, except for the streptavidin injection (2 μL/min).

Removal of Free Polymer by Size Exclusion Chromatography. SEC was performed on a fast protein liquid chromatography (FPLC) instrument (Shimadzu, Japan) equipped with a degasser (DGIU20A), a pump (LC20AI), a UV/vis detector (SPDM40), a fluorescence detector (RF20A), and fraction collector (FRC10A). Samples were loaded via an injector (Rheodyne 9725i, IDEX, USA) equipped with a 250 μL loop and eluted through a Superdex 75 10/300 column (Cytiva, Austria) at a flow rate of 0.75 mL/min. To separate nanodiscs from free polymer, 150 μL fluorescent nanodiscs at a total lipid concentration of 5 mM were injected, and the polymer and Atto 488 PE absorbance were monitored at 260 and 500 nm, respectively. Then, the first half of the exclusion peak fraction, which contained polymer and fluorescent lipid (Figure S48) was collected. Last, the lipid concentration was determined by measuring the light absorbance of fluorescent nanodiscs at 500 nm in a UV−vis spectrometer using the molar extinction coefficient of Atto-488 PE ($\varepsilon_{500\ nm}$ = 90,000 M^{-1} cm^{-1}).

Protein Extraction from Bacterial Cells. *E. coli* cells (∼2 g) were resuspended in 100 mM NaCl, 50 mM Tris, pH 8.0 (20 mL) and ultrasonicated twice for 10 min at 40% intensity, and a 0.4/0.6 s duty cycle, with 5 min cooling time between runs. All sample preparation was carried out on ice. Cell debris and unbroken cells were removed by centrifuging at 7000*g* for 10 min at 4 °C. The supernatant was ultracentrifuged at 240,000*g* for 35 min at 4 °C in a table-top ultracentrifuge (Optima Max XP) equipped with a TLA 100.3 rotor (Beckman−Coulter, Vienna, Austria). The resulting cell-membrane pellets were resuspended in PSB buffer and the ultracentrifugation step was repeated. To extract membrane proteins from the cellular membrane, pellets were resuspended in PBS supplemented with complete EDTA-free protease inhibitor and polymer stocks were added to obtain a final membrane pellet concentration of 25 mg/mL. Samples were incubated on a ThermoMixer at 800 rpm and 4 °C overnight and then ultracentrifuged at 100,000*g* and 4 °C for 80 min. The supernatant containing the solubilized protein fraction was extracted and the pellet was resuspended in 1% sodium dodecyl sulfate (SDS) in H_2O to the previous sample volume.

Analysis of Membrane Protein Extracts. All supernatant and pellet samples underwent a $CHCl_3$/MeOH precipitation as described previously.[51] The resulting dry protein pellets were resuspended in 1% SDS in H_2O and analyzed by a microplate BCA assay according to the manufacturer's instructions. Absorbance was determined in PolarStar plate reader (BMG Labtech, Ortenberg, Germany). Further, samples were subjected to SDS-PAGE analysis on precast NuPAGE 4−12% gels (Waltham, Massachusetts, USA) according to the manufacturer's instructions. Protein yields were calculated as the fraction of the total protein mass in the supernatant divided by the sum of protein masses in the supernatant and pellet fractions.

GHSR Production. The human ghrelin receptor GHSR fused to the α5 integrin and an N-terminal lanthanide binding tag was expressed in *E. coli* BL21(DE3) strain and purified from inclusion bodies.[52] Receptor folding was then carried out by adding amphipol (APol) A8−35 (Anatrace) to the SDS-solubilized receptor at a 1:5 protein/APol weight ratio in the presence of 10 μM of the JMV3011 antagonist. After 30 min incubation at room temperature, GHSR folding was initiated by precipitating dodecyl sulfate (DS) as its potassium salt through addition of KCl to a final 200 mM concentration. The potassium dodecyl sulfate (KDS) precipitate was then removed by two 30 min centrifugation steps at 15,000 rpm. The supernatant was extensively dialyzed against a 50 mM K-Phosphate, 150 mM KCl, 1 μM JMV3011, pH 8 buffer. APols were then exchanged to *n*-dodecyl-β-D-maltopyranoside (β-DDM) in the presence of cholesteryl hemisuccinate (CHS). To this end, the APol/GHSR complex was incubated for 2 h at 4 °C with 0.2% (*w*/*v*) β-DDM, 0.02% (*w*/*v*) CHS in a 50 mM Tris−HCl pH 8, 150 mM NaCl, 10 μM JMV3011 buffer. The sample was then loaded onto a pre-equilibrated 5 mL HisTrap column (Cytiva) and the resin washed with a 50 mM Tris−HCl pH 8, 150 mM NaCl, 0.2% (*w*/*v*) β-DDM, 0.02% (*w*/*v*) CHS, 10 μM JMV3011 buffer and then with 50 mM Tris−HCl pH 8, 150 mM NaCl, 0.1% (*w*/*v*) β-DDM, 0.02% (*w*/*v*) CHS, 10 μM JMV3011. The protein was eluted from the column with the same buffer containing 200 mM imidazole. Active receptor fractions were then purified using affinity chromatography. To this end, the receptor was loaded on a streptavidin-agarose column where the biotinylated JMV2959 antagonist had been bound.[53] After washing with 25 mM Na-HEPES, 150 mM NaCl, 0.1% (*w*/*v*) β-DDM, 0.02% (*w*/*v*) CHS, pH 7.4, the bound proteins were recovered by washing the column with the same buffer containing 1 mM of the JMV4183 antagonist.

MRAP2 Production. A recombinant fragment including the *N*-terminal and transmembrane domains of MRAP2 was expressed in *E. coli*. To this end, residues (1−78) of human MRAP2 fused to an *N*-terminal lanthanide-binding tag (LBT) were cloned into a pET15a expression vector (Merck). BL21(DE3) cells were transformed with the pET15a-MRAP2 plasmid and grown in Terrific Broth (TB) at 37 °C supplemented with 100 μg/mL carbenicillin. Protein expression was induced with 1 mM IPTG. After 4 h induction, cells were harvested (5000 rpm, 30 min). After resuspension in lysis buffer (50 mM Tris−HCl pH 8, containing an EDTA-free protease inhibitor cocktail), sonication and centrifugation (15,000 rpm, 40 min), inclusions bodies were solubilized in a buffer 50 mM Tris−HCl pH 8.0, 1% SDS, 10 mM imidazole and loaded on a 5 mL HisTrap column (Cytiva). IMAC purification was carried out with two washing steps at 10 mM and 20 mM imidazole, and elution at 200 mM imidazole. Detergent exchange was carried out by adding 0.1% (*w*/*v*) β-DDM, 0.02% (*w*/*v*) CHS to the protein solution. After 30 min incubation at room temperature, dodecyl sulfate was precipitated as its potassium salt through addition of KCl to a final 200 mM concentration. The KDS precipitate was then removed by two 30 min centrifugations at 15,000 rpm.

Proteoliposome Assembly and Solubilization. POPC, POPG (9:1 POPC/POPG molar ratio) and cholesterol (0.10 cholesterol/phospholipid molar ratio) in chloroform (Avanti lipids) were mixed and dried under a stream of nitrogen followed by overnight incubation under vacuum. The lipids were then solubilized in a 50 mM Na-HEPES, 100 mM NaCl, pH 7.5 buffer. After vigorous vortexing, liposomes were obtained by extrusion through a 200 nm polycarbonate filter using a mini-extruder device (Avanti Polar Lipids). Formation of LUVs was confirmed by DLS (Zetasizer Nano-ZS ZEB 3600, Malvern Instruments). Preformed liposomes were then destabilized by addition of 5 mM β-DDM and incubation for 1 h at room temperature. The β-DDM-solubilized proteins were added at protein-to-lipid ratios of 1:500 (mol/mol) and the mixture incubated for 1 h. β-DDM was removed by incubation with SM-2 Biobeads (BioRad) (10 mg of beads per mg of detergent) overnight at 4 °C, followed by an extensive dialysis in 50 mM Tris−HCl pH 8. Proteoliposomes were recovered by ultracentrifugation (100,000*g* for 30 min), resuspended in 50 mM Tris−HCl pH 8 and further purified on a 5−30% linear sucrose gradient. After extensive dialysis in a 50 mM Tris−HCl pH 8, 100 mM NaCl buffer, 2.5% (*w*/*w*) of the different polymers were added to the proteoliposomes. After overnight at 15 °C, the resulting solution was ultracentrifuged at 100,000*g* for 2 h, and the nanodiscs were recovered in the supernatant fraction. This fraction was loaded on a 1 mL HisTrap column (Cytiva), extensively washed with a 50 mM Tris−HCl, 150 mM

https://doi.org/10.1021/acsapm.5c02955
ACS Appl. Polym. Mater. XXXX, XXX, XXX−XXX

Scheme 1. Biotin-PEG$_n$-CDTPA Synthesis

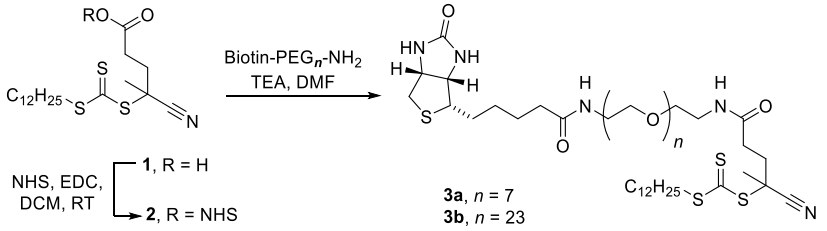

Scheme 2. SMA and Biotin-SMA Preparation by RAFT Polymerization

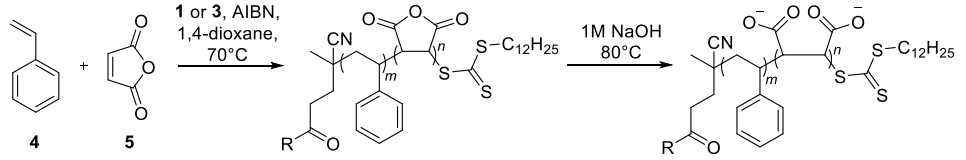

6, [m]:[n] = 3:1 ; R = OH
7, [m]:[n] = 2:1 ; R = OH
8, [m]:[n] = 3:1 ; R = Biotin-PEG$_7$-NH
9, [m]:[n] = 2:1 ; R = Biotin-PEG$_7$-NH
10, [m]:[n] = 3:1 ; R = Biotin-PEG$_{23}$-NH
11, [m]:[n] = 2:1 ; R = Biotin-PEG$_{23}$-NH

12, [m]:[n] = 3:1 ; R = OH
13, [m]:[n] = 2:1 ; R = OH
14, [m]:[n] = 3:1 ; R = Biotin-PEG$_7$-NH
15, [m]:[n] = 2:1 ; R = Biotin-PEG$_7$-NH
16, [m]:[n] = 3:1 ; R = Biotin-PEG$_{23}$-NH
17, [m]:[n] = 2:1 ; R = Biotin-PEG$_{23}$-NH

NaCl, 20 mM imidazole buffer and the protein eluted with the same buffer containing 200 mM imidazole. Homogeneous fractions of nanodiscs were finally obtained through a size-exclusion chromatography step on a S200 increase 10/300 GL column (Cytiva) using a 25 mM HEPES, 150 mM NaCl, pH 7.4 buffer as the eluent.

Protein Immobilization. The proteins were immobilized onto 96-well streptavidin coated high-capacity plates (Pierce) following manufacturer instructions. Briefly, each well was washed with 200 μL of a 25 mM Na-HEPES, 150 mM NaCl, pH 7.5, 0.1% BSA buffer. The protein was then added and incubated for 2 h at room temperature before the plates were washed. Terbium (Tb) fluorescence was then measured using a Fluoromax-4 fluorimeter (Horiba), with excitation at 280 nm and emission at 545 nm (bandwidth 5 nm).

Ligand Binding Assays. Ligand binding was monitored through the lanthanide resonance energy transfer (LRET) signal between GHSR labeled with Tb on the LBT at its *N*-terminus and a LEAP2(1−12) peptide labeled with dy647 at its C-terminus.[54] To this end, the receptor was incubated with increasing concentrations in the labeled LEAP2 peptide at 10 °C for 3 h. The LRET signal was then measured with a Fluoromax-4 fluorimeter (HORIBA) using a donor excitation at 280 nm and a signal collection at 673 nm.

Bimane Labeling and Fluorescence. GHSR-containing nanodiscs were prepared as described above using a minimal cysteine mutant of GHSR with a single reactive cysteine at position 255$^{6.27}$ (superscript numbers follow Ballesteros-Weinstein numbering).[55] The protein was labeled by incubating in the dark with a 10-fold molar excess of monobromobimane (MB) overnight at 4 °C. Labeling was stopped by adding a 100 molar excess of L-cys and incubating 1 h at 4 °C. Unreacted dye was removed by extensive dialysis. Fluorescence measurements were carried out with a Fluoromax-4 fluorimeter (HORIBA), with an excitation wavelength set at 395 nm, and emission spectra recorded between 410 and 520 nm.

RESULTS AND DISCUSSION

Approach to Synthesize SMA and Biotin-PEG$_n$-SMA Copolymers. Biotinylated SMA polymers were prepared by RAFT polymerization. The choice of the RAFT approach was based on the advantages over traditional free radical polymerization. Controlled radical polymerization using the reversible addition−fragmentation chain transfer (RAFT) method enables the synthesis of well-defined statistical copolymers with controlled molar mass and composition. The potential of RAFT-derived SMA for lipid solubilization and membrane protein extraction was first reported by Craig et al.,[18] who demonstrated that RAFT-SMA could efficiently solubilize POPC/POPG vesicles into SMALPs of different sizes. Later, Smith et al.[27] reported that RAFT-derived SMA not only solubilizes lipid mixtures with reduced dispersity in nanodisc formation compared to commercial polymers but also facilitates the efficient extraction of a GFP-tagged membrane protein.

We started with the synthesis of the CDTPA (**1**) transfer agent[49] and its modification to a biotinylated version (Scheme 1). To allow modification of the CDTPA transfer agent, we used two commercially available amino PEGylated biotin derivatives, whose PEG chains contained 7 or 23 units, that were grafted through an amide bond. It is well established that NHS functionalization is mandatory to prevent the degradation of the thiocarbonylthio function upon addition of an amino group.[42]

The terminal carboxylic acid group of CDTPA (**1**) was modified into NHS-ester group, and the resulting CDTPA-NHS was obtained without purification in almost quantitative yield (96%). CDTPA-NHS was next conjugated to the two biotin-PEG$_n$-NH$_2$ in mild reaction conditions. Purification of biotin-PEG$_7$-CDTPA (**3a**) was performed using preparative HPLC in 62% with high purity (>95%). In contrast, the PEG$_{23}$ analogue (**3b**) was purified by gravity size-exclusion chromatography (SEC) in very good yield (86%) and high purity (>97%).

The copolymerization of styrene (**4**) and maleic anhydride (**5**) was carried out in 1,4-dioxane using AIBN as radical initiator in the presence of the synthesized transfer agents (Scheme 2). We targeted a degree of polymerization of 45 for all our polymers with two different styrene/maleic anhydride ratios (3:1 and 2:1). A degree of polymerization of 45 was selected to provide polymers of sufficient length to form stable nanodiscs, while remaining short enough to ensure solubility, fast kinetics, and efficient end-group functionalization corresponding to an average molecular weight of ∼4−6 kDa. Among the various styrene/maleic anhydride (SMA) copoly-

https://doi.org/10.1021/acsapm.5c02955
ACS Appl. Polym. Mater. XXXX, XXX, XXX−XXX

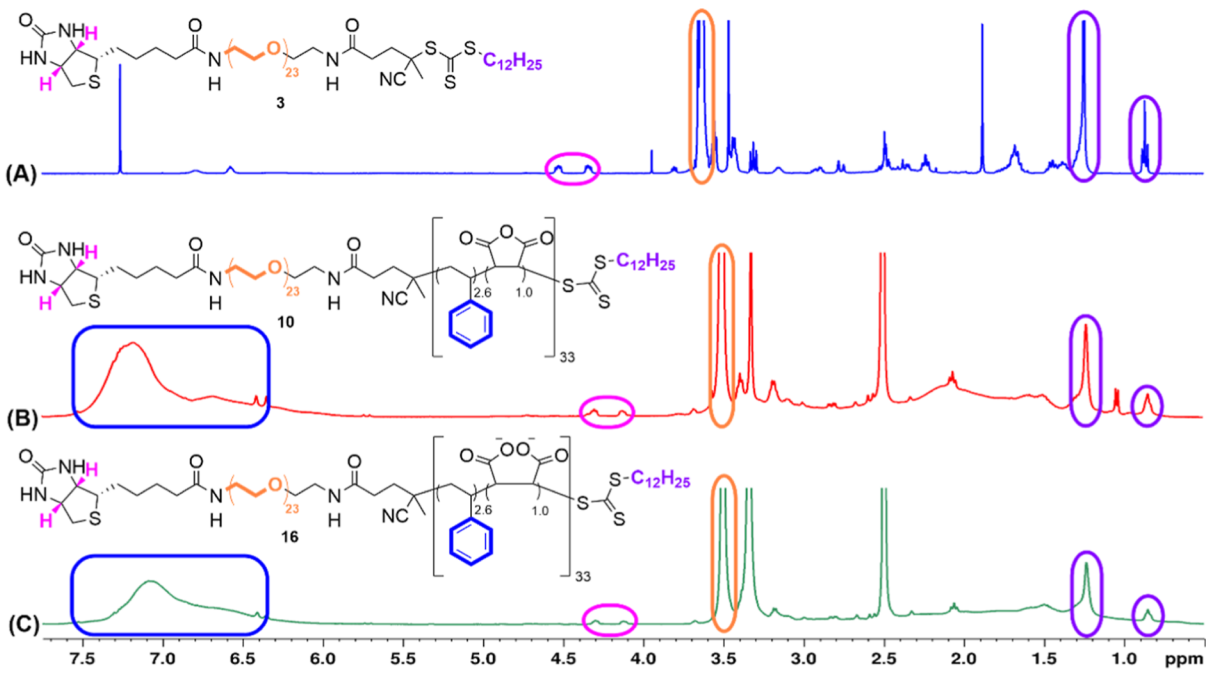

Figure 1. ^{1}H NMR spectra of: (A) Biotin-PEG$_{23}$-CDTPA (**3**), (B) Biotin-PEG$_{23}$-SMAnh (**10**), and (C) Biotin-PEG$_{23}$-SMA (**16**). Pink markers indicate protons corresponding to biotin; orange markers, the CH_2 protons of PEG groups; blue markers, protons associated with styrene; and violet markers, protons from the aliphatic chain of the CDTPA agent.

mers reported in the literature, those with styrene/maleic anhydride ratios of 2:1 and 3:1 are the most commonly utilized. These compositions are favored due to their optimal balance between hydrophobic and hydrophilic properties, which enhances their ability to interact with lipid membranes.[56] For the sake of comparison, we also prepared RAFT-SMA polymers without biotin tags. Biotin-SMAnh (**8**−**11**) exhibited characteristic signals in the ^{1}H NMR spectra, with an integrated peak area of 2 in the range of 4.0−4.5 ppm, corresponding to the vicinal hydrogens of the amide group in the biotin ring (Figure 1). Under our experimental condition, ^{1}H NMR analysis of SMAnh (**6**−**7**) and biotin-SMAnh (**8**−**11**) showed degrees of polymerization ranging from 32 to 45, close to the desired target indicating a rather good control of the polymerization. The molar masses determined by SEC and ^{1}H NMR were in good agreement, although no clear tendency was noted. The discrepancies observed are inherent to the application of a nonuniversal SEC calibration (polystyrene standards) and the subsequent lower size (hydrodynamic volume) of SMAnh compared to polystyrene.

The dispersity ($Đ$) of SMAnh polymers obtained through free radical polymerization is typically in the range of 2.0−2.5,[57] while in our hand RAFT polymerization led to significantly lower $Đ$ around 1.20 (Table 1), in agreement with the previously reported RAFT-SMA polymers ($Đ \sim$ 1.30).[18] We recently reported PET-RAFT SMA polymer with $Đ$ close to 1.1.[58] A higher $Đ$, indicating a broader molar mass distribution, generally leads to greater variability in nanodisc size. In contrast, a lower $Đ$, characteristic of more uniform polymers, tends to produce nanodiscs with more consistent diameters.[27,29]

A hydrolysis step was carried out using NaOH to convert maleic anhydride into maleic acid, rendering the final polymers water-soluble. The SMAs (**12**−**17**) were purified by dialysis using membranes with 1 kDa molecular weight cutoff, and water was removed by lyophilization. The resulting hydrolyzed polymers were further subjected to structural characterization by ^{1}H NMR. The hydrolyzed biotin-SMA polymers (**14**−**17**) exhibited the characteristic peaks of the biotin moiety (Figure 1). Degrees of polymerization were also determined by ^{1}H NMR and varied between 31 and 45, in excellent agreement with those determined for the nonhydrolyzed polymers.

In addition, whatever the transfer agent chosen (CDTPA or biotin-modified CDTPA) we observed a good correlation between the monomer ratio initially chosen and the final ratio in the polymer as determined by ^{1}H NMR (Table 1). Similarly, after hydrolysis of the maleic anhydride groups we confirmed the integrity of the polymer chain ends obtained, as evidenced by the good correlation between the styrene to maleic anhydride and the styrene to maleic acid ratios measured by ^{1}H NMR (Table 1).

Behavior of Polymers in Aqueous Solution. The SMAs (**12**−**17**) were subjected to dynamic light scattering (DLS) analysis in aqueous medium. The diameter of the micelles varied between 9 and 13 nm on average, corroborating the results of SMA synthesized via RAFT in the literature.[29,58] It is worth noting that neither the PEG$_7$ nor PEG$_{23}$ group linked to the end of the polymer chain significantly affected the diameter of the objects (see results Table 1 and Figure S44). Recent reports have studied the effect of end-group of RAFT-SMA polymers. While Edler and co-workers concluded that the size of the aggregates was mainly influenced by the diblock structure and overall composition of the polymer rather than by the nature of the end-group (a C12 chain vs a CN group),[29] Farrelly et al. noted differences between a polymer bearing a COOH end group and a polymer whose end group was cleaved.[30]

Lipid-Solubilization Efficiency of Biotinylated SMA(2:1). We characterized the lipid-solubilization efficiency of biotinylated SMA by performing titrating large unilamellar vesicles (LUVs) composed of 1,2-dimyristoyl-*sn*-glycero-3-

https://doi.org/10.1021/acsapm.5c02955
ACS Appl. Polym. Mater. XXXX, XXX, XXX−XXX

Table 1. SMAnh. (6-7), Biotin-SMAnh (8-11), SMA (14-13) and Biotin-SMA (14-17) Data

polymer		batch	conversion styrene[a]	F_S[b]	[St]/[MAnh]	DP_n[c]	M_n (RMN)[d] g mol^{-1}	M_n (SEC)[e] g mol^{-1}	M_w (SEC)[e] g mol^{-1}	$Đ$[e]	polymer		batch	F_S[b]	[St]/[MA]	DP_n[c]	M_n (RMN)[f] g mol^{-1}	size[g] (nm)
SMAnh	**6a**	MG28	80%	0.74	[2.9]: [1.0]	39	4353	3392	4218	1.24	SMA	**12a**	MG30	0.76	[3.2]: [1.0]	38	4445	12.8 ± 4.5
	6b	MG35	81%	0.75	[3.0]: [1.0]	36	4093	3448	4198	1.21		**12b**	MG37	0.76	[3.4]: [1.0]	35	4191	13.1 ± 4.3
	7a	MG46	79%	0.69	[2.3]: [1.0]	39	4386	3311	4001	1.20		**13a**	MG48	0.68	[2.1]: [1.0]	37	4337	9.9 ± 2.9
	7b	MG51	77%	0.70	[2.2]: [1.0]	42	4705	2940	3787	1.28		**13b**	MG53	0.70	[2.2]: [1.0]	42	4913	9.7 ± 3.7
biotin-PEG_7-SMAnh	**8a**	MG29	79%	0.78	[3.1]: [1.0]	37	4713	6293	7105	1.12	biotin-PEG_7-SMA	**14a**	MG31	0.77	[3.5]: [1.0]	36	4820	12.1 ± 4.1
	8b	MG36	74%	0.76	[3.4]: [1.0]	35	4544	5785	6747	1.16		**14b**	MG38	0.78	[3.7]: [1.0]	33	4549	16.1 ± 5.5
	9a	MG47	56%	0.66	[1.8]: [1.0]	32	4274	2829	3882	1.37		**15a**	MG49	0.68	[2.1]: [1.0]	31	4378	7.6 ± 5.2
	9b	MG52	71%	0.67	[2.0]: [1.0]	45	5561	3775	5139	1.36		**15b**	MG54	0.65	[1.8]: [1.0]	45	5910	8.6 ± 3.2
biotin-PEG_{23}-SMAnh	**10**	MG103	72%	0.72	[2.7]: [1.0]	33	5037	4582	5172	1.12	biotin-PEG_{23}-SMA	**16**	MG104	0.72	[2.7]: [1.0]	33	5178	9.4 ± 3.3
	11a	MG100	80%	0.69	[2.2]: [1.0]	35	5209	5064	5839	1.15		**17a**	MG101	0.70	[2.4]: [1.0]	34	5355	9.8 ± 5.0
	11b	MG106	78%	0.64	[1.8]: [1.0]	42	5908	4589	5294	1.15		**17b**	MG107	0.65	[1.9]: [1.0]	40	6036	11.1 ± 3.9

[a]Conversion calculated by ^{1}H NMR using 1,3,5-Trioxane as internal calibrant. Maleic anhydride conversion was not determined due to an overlap of specific proton and that of the polymer chain. [b]$Fs = \int phenyl\_region \times 0.2/((\int aliph\_region - \int CTA\_aliph\_region) \times 0.5 - \int phenyl\_region \times 0.1)$ with $\int CTA\ aliph.$ region = 29 for CDTPA, 72 for biotin-PEG_7-CDTPA and 136 for biotin-PEG_{23}-CDTPA. [c]$DP_n = DP_n$ (styrene) + DP_n(MAnh); $DP_n(\text{styrene}) = (\int phenyl\_region)/5$; $DP_n(\text{MAnh}) = (\int aliph\_region - \int phenyl\_region \times 3/5 - \int CTA\_aliph\_region)/2$. [d]$M_n = DP_n \times Fs \times 104 + DP_n \times (1\ Fs) \times 98 + MW(CTA)$; MW(CTA) = 403 g/mol for SMAnh, 980.5 g/mol for biotin-PEG_7-SMAnh and 1685 g/mol for biotin-PEG_{23}-SMAnh. [e]Determined by size exclusion chromatography in *N,N*-dimethylformamide with 0.05 M LiBr, calibrated with polystyrene standards. [f]$M_n = DP_n \times Fs \times 104 + DP_n \times (1\ Fs) \times 116 + MW(CTA)$; MW(CTA) = 403 g/mol for SMA, 980.5 g/mol for Biotin-PEG_7-SMA and 1685 g/mol for Biotin-PEG_{23}-SMA. [g]Hydrodynamic particle size distribution of polymers measured in PBS (pH 7.4).

https://doi.org/10.1021/acsapm.5c02955
ACS Appl. Polym. Mater. XXXX, XXX, XXX−XXX

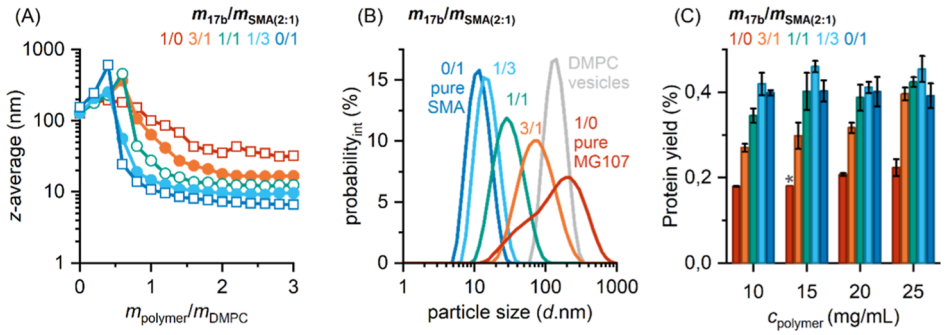

Figure 2. Solubilization of lipid vesicles by **17b** and **17b**/SMA(2:1) mixtures. (A) *z*-Average particle size derived from DLS as a function of polymer/lipid mass ratio. Vertical bars are not error bars but indicate the peak width of the particle size distribution as given by $\sigma = \sqrt{\text{PDI}}\,z$, with PDI being the polydispersity index and *z* the *z*-average particle diameter. (B) Intensity-weighted particle size distributions of **17b**, SMA(2:1), and **17b**/SMA(2:1) mixtures added to DMPC vesicles at a polymer/lipid mass ratio of 1, as obtained from DLS. (C) Protein yield from *E. coli* membrane preparations treated with **17b**/SMA(2:1) mixtures, as determined by a colorimetric protein concentration assay. Samples were prepared in triplicates, except one data point without any replicates, which is marked with a star.

phosphocholine (DMPC) with polymers. Then, we monitored the formation of nanodiscs by analyzing the particle sizes at increasing polymer/lipid mass ratios ($m_{polymer}/m_{DMPC}$, Figure 2A) for different mixtures of biotinylated polymer **17b** and nonbiotinylated SMA(2:1).

Pure **17b** produced large, polydisperse lipid particles at high polymer/lipid ratios. Interestingly, we found that **17b** alone caused an initial increase in particle sizes at polymer/lipid ratios <0.6, followed by a steady decrease in particle diameter down to 35 nm at a polymer/lipid ratio of 3. Pure **15b** exhibited a similar behavior, with an increase in particle size up to a polymer/lipid ratio of 1.2 and a decrease down to about 20 nm at polymer/lipid mass ratio of 3 (Figure S45). This indicates the length of the PEG moiety (7 units for **15b** and 23 units for **17b**) has no significant effect on the capacity to solubilize DMPC membranes. This is in contrast with SMA(2:1), which caused a sharp increase in size up to 537 nm with final particle sizes <20 nm at polymer/lipid ratio below 0.8. Particle size distributions at a polymer/lipid ratio of 1 show that SMA(2:1) solubilized the vesicles completely, whereas **17b** produced a significant amount of aggregates. We also tested the 3:1 polymers. While pure **14b** showed no change in particle diameter, SMA(3:1) showed a similar behavior as SMA(2:1) (Figure S45).

Supplementing Biotinylated Polymers with SMA Enables Efficient Nanodisc Formation. To produce nanodiscs with high efficiency while incorporating biotinylated SMA in the polymer belt, we decided to repeat the experiment with mixtures of **17b** and nonbiotinylated SMA(2:1). We thus found that mixtures containing equal masses of both polymers solubilized vesicles and reduced the *z*-average particle diameter to 18.1 nm at a polymer/lipid mass ratio of 1. We observed a nearly identical trend for the SMA(2:1) variant **15b** (Figure S45). For the SMA(3:1) variant **14b**, which did not solubilize vesicles on its own, we could restore the solubilization efficiency by supplementing SMA(3:1) (Figure S45). In all cases, a mass ratio of nonbiotinylated to biotinylated polymer of 1 sufficed to solubilize vesicles efficiently. Of note, mixtures of nonbiotinylated and biotinylated polymers produced nanodiscs exhibiting a 2-fold increase in size compared with nanodiscs made from nonbiotinylated alone.

Protein Solubilization. We next tested the potency of the polymers to solubilize membrane proteins. First, we investigated the use of biotinylated SMA for total membrane protein extraction from *E. coli* membranes. To this end, bacterial membrane fractions were titrated with polymer, followed by separation of polymer-extracted from nonsolubilized protein by ultracentrifugation. We observed a similar trend as for the solubilization of pure lipid vesicles: pure biotinylated SMA could achieve a protein extraction efficiency of ∼20%, which significantly improved up to 40% upon the addition of commercially available, nonbiotinylated SMA (Figures 2C and S46). Next, we used two model proteins with different structural organization, namely, a monotopic transmembrane protein, MRAP2, and a polytopic receptor, GHSR. MRAP2 is a protein with a single-pass transmembrane helix and has been shown to modulate the signaling properties of the melanocortin receptors.[59] In contrast, GHSR is a G protein-coupled receptor (GPCR) with a typical seven transmembrane helix fold.[60] Both proteins were expressed with a lanthanide-binding tag (LBT) at their *N*-terminus in *E. coli* inclusion bodies and refolded in vitro in detergent solutions. To analyze the ability of the polymers to solubilize these proteins from a lipid-bilayer environment, GHSR and MRAP2 were first assembled into 200 nm liposomes composed of POPC/POPG (9:1 molar ratio) containing cholesterol (10% molar ratio). DMPC has previously been shown to negatively impact the functional properties of GHSR.[53] These proteoliposomes were then incubated with 2.5% of the different polymers. For the sake of comparison, we included SMA(3:1) and DIBMA. Based on our previous data with functionalized amphipols[44] and the results obtained in the lipid-solubilization assay (see above), 1:1 mixtures of biotinylated and nonbiotinylated polymers were used in each case. Solubilization efficiency was then calculated from the intensity of the emission of Terbium (Tb) bound to the LBT in the soluble fraction after incubation with the polymers compared to the initial value in the liposomes. As shown in Figure 3, solubilization ratios in the 20−30% range were obtained whatever the polymer tested, with a ratio systematic larger for MRAP2 than for GHSR. This suggests that, under the present conditions, solubilization efficiency may depend, at least to some extent, on the topological features of the protein. Among the polymers tested, SMA(3:1) and DIBMA were the most and least efficient solubilizers, respectively, while no significant differences were noted between the 2:1 and the 3:1 variants of the new biotinylated SMA polymers.

https://doi.org/10.1021/acsapm.5c02955
ACS Appl. Polym. Mater. XXXX, XXX, XXX−XXX

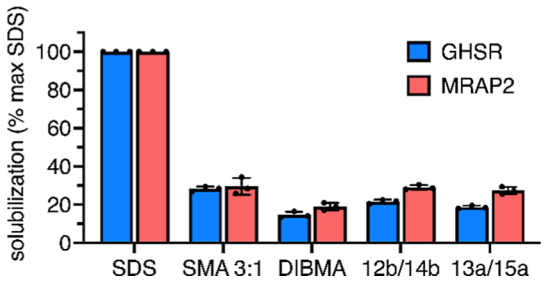

Figure 3. Solubilization yields. Solubilization ratios correspond to the ratio of solubilized protein after o/n incubation of the GHSR or MRAP2 containing liposomes with 2.5% (*w*/*w*) normalized to the amount of protein solubilized with 5% SDS. Data are means ± SDs of three measurements.

Functional Properties of the Solubilized Proteins. After solubilization of proteoliposomes with the different polymers, extracted proteins were purified through two successive IMAC and SEC steps to remove unsolubilized proteins, empty nanodiscs, and excess free polymer. The functional properties of the resulting protein fractions were then evaluated. This was limited to GHSR, however, as MRAP2 has no functional readout besides its ability to affect the signaling properties of its receptor partner. For GHSR, we assessed the ability of the receptor to bind a fluorescent derivative of the *N*-terminal part of the natural inverse agonist LEAP2 (dy647-LEAP2(1−12)).[54] As shown in Figure 4, the

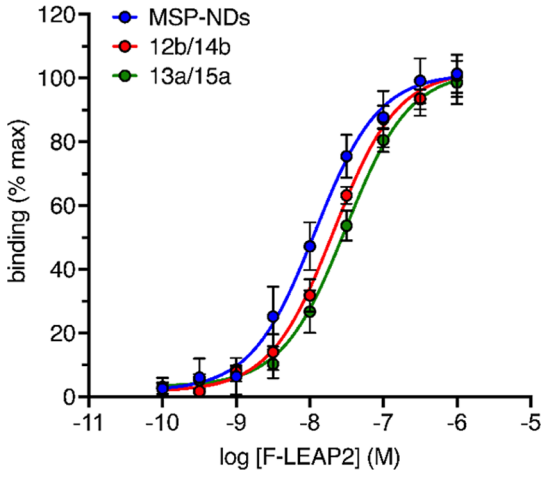

Figure 4. Binding of fluorescent LEAP2 to isolated GHSR in nanodiscs encapsulated by biotinylated SMA polymers or MSP. Binding was monitored through the FRET signal between Tb bound to the LBT of the receptor and the dy647 moiety attached to the C-terminus of the LEAP2(1−12) analog. Data are normalized to the maximum signal and are the mean ± SD of three measurements.

receptor in biotinylated SMA nanodiscs bound this ligand with an affinity similar to that measured for the same receptor in nanodiscs stabilized by the membrane scaffold protein (MSP) MSPE3D1. These latter nanodiscs were used as a reference as we have previously shown that they fully preserve the functional properties of GHSR.[52] Hence, this direct comparison indicates that solubilization in a mixture of biotinylated/nonbiotinylated SMAs has no detrimental impact on the function of GHSR, at least as far as ligand binding is concerned.

Surface Plasmon Resonance with Biotinylated Nanodiscs. Next, we investigated the immobilization of biotinylated nanodiscs by means of surface plasmon resonance (SPR) spectroscopy. Immobilizing nanodiscs via their polymer belt would allow surface-bound analysis methods such as SPR binding assays, ELISA protocols, and TIRF microscopy using polymer-encapsulated nanodiscs containing unmodified membrane proteins. Thus, these analyses could be performed without adding affinity tags to the target protein, thereby avoiding possible complications resulting from attaching tags to the protein.

First, we probed the binding of **17b**/SMA(2:1) nanodiscs containing DMPC to a streptavidin-decorated SPR chip. We found that mixtures of biotinylated polymers and biotin-free SMA produced nanodiscs with streptavidin affinity, whereas the nonbiotinylated control sample showed negligible unspecific binding to the SPR chip. In addition, the slow, quasi-linear dissociation of biotinylated nanodiscs after injection (Figure 5A) suggests that nanodiscs were stably bound under SPR buffer flow. These data demonstrate that biotinylated, polymer-encapsulated nanodiscs are suitable for SPR analysis, as they bind with high affinity and specificity.

Removal of Free Polymer for SPR. Next, we tested the influence of free, unbound polymer on nanodisc immobilization. To this end, we produced nanodiscs containing a small fraction (0.5 mol %) of fluorescently labeled lipids and performed two SPR series. First, we probed a concentration series of nanodiscs in a multicycle SPR measurement. Second, we performed size exclusion chromatography (SEC) to remove free, unbound polymer from the nanodiscs and then repeated the SPR experiment with identical parameters (Figure S47). Using fluorescent lipids was essential to separately follow the elution of lipid and polymer in SEC and to normalize the lipid concentrations between the two SPR experiments. Strikingly, the SPR signal was increased by a factor of 2 for SEC-purified nanodiscs as compared with unpurified nanodiscs (Figure 5D). This signal increase implies that free, biotinylated polymer chains might compete with nanodiscs for streptavidin binding sites, thus lowering the nanodisc coverage. To test this hypothesis, we added a final injection of 1 mM SDS to our standard SPR protocol (Figure S47); while SDS will not disrupt the biotin−streptavidin interaction, it will disintegrate lipid-bilayer nanodiscs. Thus, an SDS injection should reduce the SPR response more severely for immobilized nanodiscs than for lipid-free polymer chains. Indeed, we observed that the signal for SEC-purified nanodiscs decreased 4-fold compared with the control (Figure 5E). This suggests that even a small fraction of free polymer can adversely affect the coverage of streptavidin-coated SPR chips with biotinylated nanodiscs. However, this unwanted effect can be reduced by a single SEC step using a commercial column prior to SPR analysis.

Binding of Protein-Containing Nanodiscs to Streptavidin. Finally, we analyzed whether the two model proteins GHSR and MRAP2 when embedded into nanodiscs could be immobilized onto streptavidin surfaces. To this end, immobilization on streptavidin-coated plates was carried out under standard conditions (see Material and Methods section). We estimated the amount of protein immobilized under such conditions by measuring the emission intensity of Tb bound to the target protein LBT after immobilization. Under such conditions, 20−30% of the emission signal initially present was recovered on the streptavidin plates for both GHSR and

https://doi.org/10.1021/acsapm.5c02955
ACS Appl. Polym. Mater. XXXX, XXX, XXX−XXX

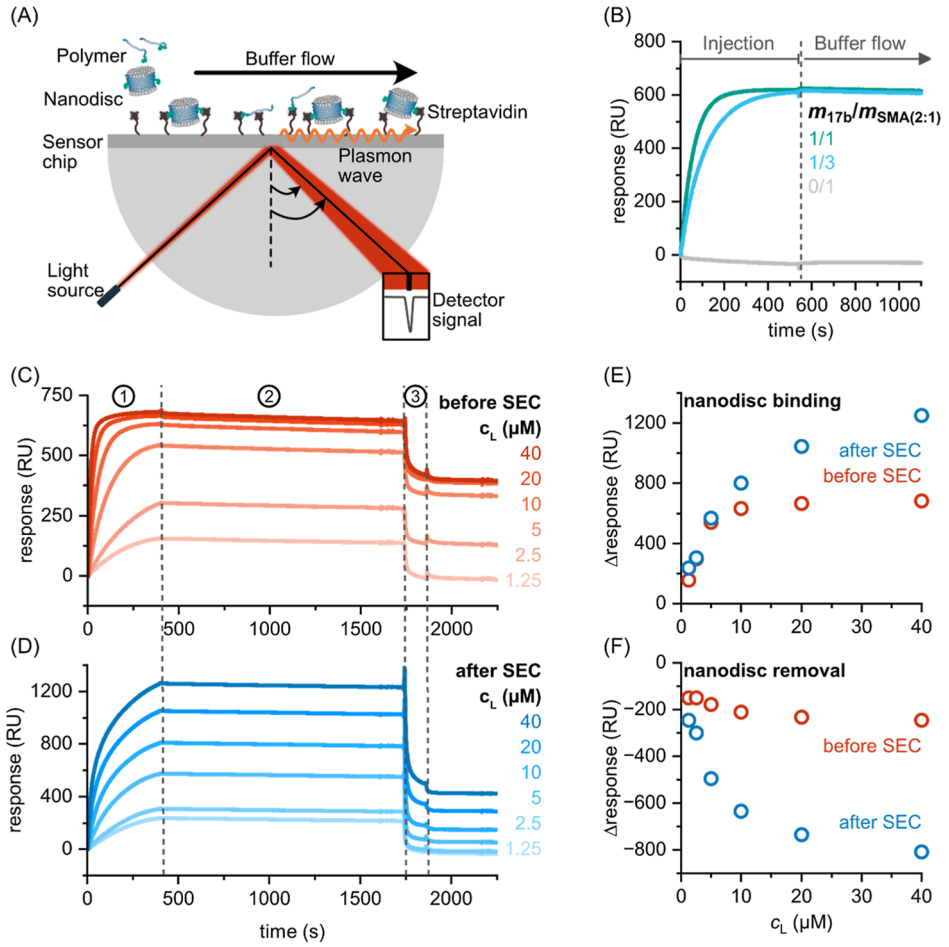

Figure 5. Immobilization of biotinylated nanodiscs encapsulated by **17b**/SMA(2:1) for surface plasmon resonance (SPR) analysis. (A) Principle of SPR analysis. Nanodiscs are injected over a streptavidin-coated gold chip. Upon nanodisc binding, a local change in refractive index causes a shift in the SPR signal, which is proportional to the amount of analyte bound to the chip. (B) Binding specificity of biotinylated nanodiscs to streptavidin-coated surfaces. (C) Concentration series of biotinylated nanodiscs before purification by SEC, numbers indicate the periods for 1: Nanodisc injection, 2: Buffer flow after nanodisc binding, and 3: Injection of 1 mM SDS. (D) Concentration series with identical parameters as in (C) performed with SEC-purified nanodiscs. Note that the *y*-axis is rescaled to show the higher instrument response to purified nanodiscs. (E) SPR response delta, derived from the signal levels before and after the injection of biotinylated nanodiscs without (red) or with (blue) SEC purification. (F) SPR response delta, derived from the signal levels before and after the injection of 1 mM SDS to immobilized nanodiscs without (red) or with (blue) SEC purification.

MRAP2 (Figure 6), indicative of immobilization yields in this same range. In contrast to solubilization, no significant difference was observed between GHSR and MRAP2 with regard to the immobilization efficiency, suggesting that the topology of the protein has no major impact on the immobilization through the biotinylated SMA belt.

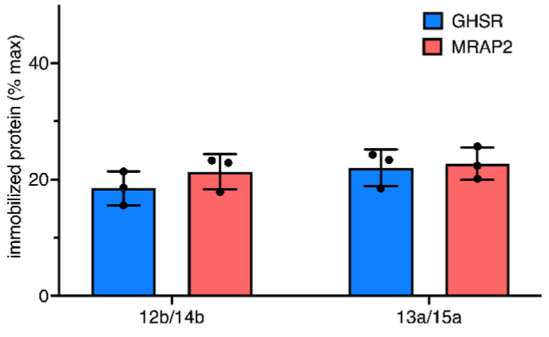

Figure 6. Immobilization ratio for GHSR and MRAP2 in the different polymer mixtures used. This ratio is that of the emission intensity of Tb bound to the LBT of the protein attached to the streptavidin plates after washing to that before immobilization. Data are means ± SDs of three experiments.

We also wondered if the immobilization process might affect the functional properties of embedded membrane proteins. Again, this was carried out only for the GHSR, as no functional readout is available for MRAP2. We first monitored ligand binding using the FRET-based assay described above. As shown in Figure 7A, the binding profiles obtained were very similar to those of the nonimmobilized receptor. Only a slight decrease in the affinity of the receptor immobilized with the aid of the 2:1 variant polymers **13a**/**15a** for the LEAP2 analog was observed. We then monitored GHSR activation through the emission properties of the fluorophore monobromobimane (MB) attached to C255.[6.27] When MB is located at this position, fluorescence changes primarily report on the clockwise movements of TM6, which are a hallmark of GPCR activation.[61] As shown in Figure 7B, the emission properties of MB were very similar for free and immobilized GHSR, whatever the ligand was. Altogether, these data suggest that immobilization onto the streptavidin surface through the

https://doi.org/10.1021/acsapm.5c02955
ACS Appl. Polym. Mater. XXXX, XXX, XXX−XXX

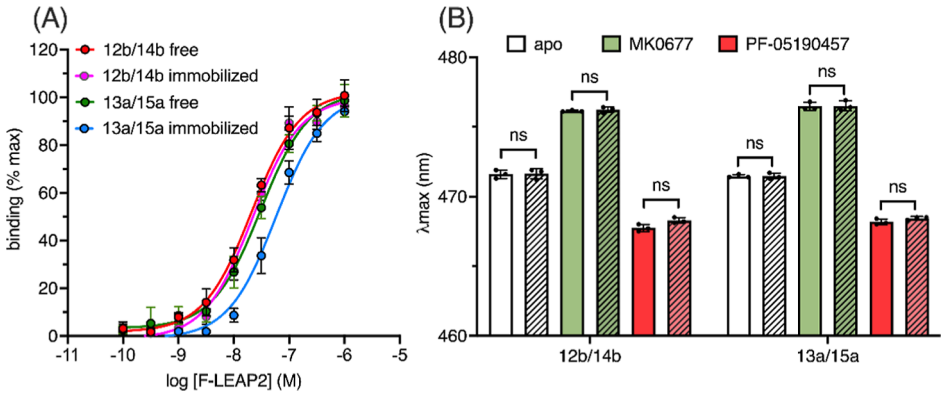

Figure 7. Pharmacological properties of the immobilized ghrelin receptor. (A) FRET-monitored binding of dy647-LEAP2(**1**−**12**) to the isolated GHSR free in solution or immobilized on the streptavidin plates. Data were normalized to the maximum signal. (B) Maximum emission wavelength (λ_{max}) of MB attached to C255$^{6.27}$ in the absence of ligand (apo), in the presence of 10 μM of the full agonist MK0677 or in the presence of 10 μM of the inverse agonist PF-05190457 free in solution (plain bars) or immobilized on streptavidin plates (hatched bars). In all cases, data are the mean ± SD of three measurements. Statistical values in (B) were obtained by means of unpaired Student's *t*-test (ns not significant).

polymer belt does not impair the pharmacological properties of the ghrelin receptor in a major way, as far as ligand binding and receptor activation are concerned.

Discussion on the Strategy for Immobilizing Membrane Proteins on Surface. The strategy based on affinity tag conjugation has been commonly employed to immobilize membrane proteins.[35] The coating of amphiphilic polymers that stabilize membrane proteins such as amphipols or nanodisc-forming amphiphilic copolymers is a promising method. However, when comparing postfunctionalization of the polymer to the functionalization of the transfer agent, caution is advised, as the former can lead to heterogeneous labeling, reduced control over functional group placement, and potential variability in polymer performance. For example, one limitation of tagged A8−35 amphipol is the random distribution of the tag along the polymer chain, as the synthesis protocol does not allow precise control over its placement.[45] This lack of specificity may affect the immobilization of the complex. To overcome this drawback, biotinylated phosphorylcholine amphipols (B-PCAPols) were synthesized using RAFT polymerization, incorporating a transfer agent to which the biotin group was subsequently grafted.[43] This approach ensured the attachment of a single biotin moiety at the polymer chain terminus. However, the synthesis of these polymers is complex, limiting their large-scale production. Additionally, amphipols with ionic or phosphorylcholine-based functionalities exhibit a high electrostatic charge density, which can lead to nonspecific binding or electrostatic repulsion.[62] To overcome ionic interactions when analyzing protein−ligand interactions, biotinylated nonionic amphipols (BNAPols) were further developed by our group.[44] However, amphipols still face limitations compared to nanodisc-forming polymers such as SMA, as amphipols lack a native-like lipid-bilayer environment and may not preserve the full structural and functional integrity of membrane proteins.

Therefore, the immobilization of lipid nanodisc has been of increasing interest. Lindhoud et al. first described a commercial SMA 2:1 copolymer grafted with cysteamine via amide formation at the maleic acid moiety.[63] They produced lipid nanodiscs and subsequently functionalized them with biotin-maleimide or maleimide-PEG$_{11}$-biotin through thiol−ene click chemistry, resulting in heterogeneity in the grafting with some polymers containing multiple sulfhydryl groups, while others had none. Very recently, the specific binding of SMALPs onto gold surface was reported with polymers bearing a trithiocarbonate end-group. However, nonspecific binding was also observed with polymers lacking this end group.[30]

In this work, we successfully employed the RAFT polymerization methodology, ensuring that the transfer agent functions as the terminal group of the polymer chains, thereby guaranteeing that all chains contain a biotin moiety. This strategy enhances homogeneity compared to postfunctionalization and allow efficient immobilization of nanodiscs with high specificity. Further, we found that free, unbound biotinylated polymer chains compete with nanodiscs for streptavidin binding sites, which can be avoided by separating nanodiscs and free polymers with the aid of SEC. Thus, we could establish a simple workflow to produce and immobilize nanodiscs on an SPR sensor chip without the need to modify the protein or lipid content of the nanodiscs. This new workflow might be expanded to any surface-based analysis of nanodisc-embedded proteins.

CONCLUSION

In this study, we synthesized a library of biotinylated SMA copolymers via RAFT polymerization using PEG-biotin-functionalized transfer agents. This strategy allowed for precise and consistent end-group functionalization, resulting in polymers that retain membrane-solubilization capacity and nanodisc-forming ability when mixed with nonbiotinylated SMA. These biotinylated lipid-bilayer nanodiscs can efficiently and specifically be immobilized onto surfaces via biotin−streptavidin interactions, paving the way for downstream biosensing applications. This approach provides a valuable tool for the study of membrane proteins in their native lipid environment, offering improved reproducibility, modularity, and compatibility with surface-based analytical techniques. Future work may explore the integration of these functionalized nanodiscs with diverse membrane-protein targets and detection platforms to expand their utility in drug discovery and diagnostics.

https://doi.org/10.1021/acsapm.5c02955
ACS Appl. Polym. Mater. XXXX, XXX, XXX−XXX

■ ASSOCIATED CONTENT

Supporting Information

The Supporting Information is available free of charge at https://pubs.acs.org/doi/10.1021/acsapm.5c02955.

^{1}H and ^{13}C NMR spectra of compounds **2** and **3a−3b**; ^{1}H NMR of polymers **6−17**; HPLC profiles and HR-MS of compounds **3a−3b**; Size exclusion chromatograph MW distribution of polymers **6−17**; DLS of polymers **12−17**, DLS of DMPC lipid vesicles treated with polymers **14b** and **15**; *E. coli* membrane protein extraction with polymers **14b**, **15b** and pure SMA; SPR protocols with SMA polymer; Size exclusion chromatography of nanodiscs (PDF)

■ AUTHOR INFORMATION

Corresponding Author

Grégory Durand − *Avignon Université, ERIT S2CB, UPRI, Avignon F-84000, France;* orcid.org/0000-0001-6680-2821; Email: gregory.durand@univ-avignon.fr

Authors

Marco Antônio G. B. Gomes − *Avignon Université, ERIT S2CB, UPRI, Avignon F-84000, France;* orcid.org/0000-0002-6494-3804

David Glueck − *Biophysics, Institute of Molecular Biosciences (IMB), NAWI Graz, University of Graz, 8010 Graz, Austria; Field of Excellence BioHealth, University of Graz, 8010 Graz, Austria; BioTechMed-Graz, 8010 Graz, Austria;* Present Address: Institute of Biochemistry, Biocenter, Goethe University Frankfurt, Max-von-Laue-Str. 9, 60438 Frankfurt am Main, Germany

Valentin Monjal − *Avignon Université, ERIT S2CB, UPRI, Avignon F-84000, France*

Marjorie Damian − *Institut des Biomolécules Max Mousseron IBMM, Univ Montpellier, CNRS, ENSCM, Montpellier 34293, France*

Pierre Guillet − *Avignon Université, ERIT S2CB, UPRI, Avignon F-84000, France*

Jean-Louis Banères − *Institut des Biomolécules Max Mousseron IBMM, Univ Montpellier, CNRS, ENSCM, Montpellier 34293, France;* orcid.org/0000-0001-7078-1285

Sandro Keller − *Biophysics, Institute of Molecular Biosciences (IMB), NAWI Graz, University of Graz, 8010 Graz, Austria; Field of Excellence BioHealth, University of Graz, 8010 Graz, Austria; BioTechMed-Graz, 8010 Graz, Austria;* orcid.org/0000-0001-5469-8772

Complete contact information is available at: https://pubs.acs.org/10.1021/acsapm.5c02955

Author Contributions

Marco Antônio G. B. Gomes, investigation, writing—original draft; David Glueck, investigation, writing—original draft; Valentin Monjal, methodology; Marjorie Damian, investigation; Pierre Guillet, methodology, supervision; Jean-Louis Banères, funding acquisition, methodology, supervision, writing—review and editing; Sandro Keller, funding acquisition, methodology, supervision, writing—review and editing; Grégory Durand, funding acquisition, methodology, project administration, supervision, writing—original draft, writing—review and editing.

Notes

The authors declare no competing financial interest.

■ ACKNOWLEDGMENTS

This work received support from the Agence Nationale de la Recherche (ANR) through grant ANR-20-CE92-0028. V.M. was the recipient of a Postdoctoral grant from the "Région Provence Alpes Côte d'Azur" and the company CALIXAR (France). We acknowledge the financial support of the European Regional Development Fund, the French government, the "Région Provence Alpes Côte d'Azur", the "Département de Vaucluse" and the "Communauté d'agglomération grand Avignon" for access to the NMR platform (CPER 3A).

■ ABBREVIATIONS

AIBN, 2,2′-azobis(2-methylpropionitrile); APols, amphiphilic polymers; CDTPA, 4-cyano-4-[(dodecylsulfanylthiocarbonyl)-sulfanyl]pentanoic acid; DLS, dynamic light scattering; DMF, *N*,*N*-Dimethylformamide; EDC, 1-ethyl-3-(3-(dimethylamino)propyl)carbodiimide; MA, maleic acid; MAnh, anhydride maleic; MB, monobromobimane; NHS, *N*-hydroxysuccinimide; NMR, nuclear magnetic resonance; RAFT, reversible addition−fragmentation chain-transfer; SEC, size exclusion chromatography; SMA, poly(styrene-*co*-maleic acid); SMALP, poly(styrene-*co*-maleic acid) lipid particles; SMAnh, poly(styrene-*co*-maleic anhydride); St, Styrene; PEG, polyethylene glycol.

■ REFERENCES

(1) Overington, J. P.; Al-Lazikani, B.; Hopkins, A. L. How many drug targets are there? *Nat. Rev. Drug Discovery* **2006**, *5* (12), 993−996.

(2) Fagerberg, L.; Jonasson, K.; von Heijne, G.; Uhlén, M.; Berglund, L. Prediction of the human membrane proteome. *Proteomics* **2010**, *10* (6), 1141−1149.

(3) Garavito, R. M.; Ferguson-Miller, S. Detergents as tools in membrane biochemistry. *J. Biol. Chem.* **2001**, *276*, 32403−32406.

(4) Zhang, Q.; Tao, H.; Hong, W.-X. New amphiphiles for membrane protein structural biology. *Methods* **2011**, *55* (4), 318−323.

(5) Hovers, J.; Potschies, M.; Polidori, A.; Pucci, B.; Raynal, S.; Bonneté, F.; Serrano-Vega, M. J.; Tate, C. G.; Picot, D.; Pierre, Y.; Popot, J. L.; Nehmé, R.; Bidet, M.; Mus-Veteau, I.; Bußkamp, H.; Jung, K.-H.; Marx, A.; Timmins, P. A.; Welte, W. A class of mild surfactants that keep integral membrane proteins water-soluble for functional studies and crystallization. *Mol. Membr. Biol.* **2011**, *28* (3), 171−181.

(6) Soulié, M.; Deletraz, A.; Wehbie, M.; Mahler, F.; Bouchemal, I.; Le Roy, A.; Petit-Härtlein, I.; Keller, S.; Meister, A.; Pebay-Peyroula, E.; Breyton, C.; Ebel, C.; Durand, G. Zwitterionic fluorinated detergents: From design to membrane protein applications. *Biochimie* **2023**, *205*, 40−52.

(7) Wehbie, M.; Onyia, K. K.; Mahler, F.; Le Roy, A.; Deletraz, A.; Bouchemal, I.; Vargas, C.; Babalola, J. O.; Breyton, C.; Ebel, C.; Keller, S.; Durand, G. Maltose-Based Fluorinated Surfactants for Membrane-Protein Extraction and Stabilization. *Langmuir* **2021**, *37* (6), 2111−2122.

(8) Chae, P. S.; Rasmussen, S. G. F.; Rana, R. R.; Gotfryd, K.; Chandra, R.; Goren, M. A.; Kruse, A. C.; Nurva, S.; Loland, C. J.; Pierre, Y.; Drew, D.; Popot, J.-L.; Picot, D.; Fox, B. G.; Guan, L.; Gether, U.; Byrne, B.; Kobilka, B.; Gellman, S. H. Maltose-neopentyl glycol (MNG) amphiphiles for solubilization, stabilization and crystallization of membrane proteins. *Nat. Meth.* **2010**, *7* (12), 1003−1008.

(9) Chae, P. S.; Gotfryd, K.; Pacyna, J.; Miercke, L. J. W.; Rasmussen, S. G. F.; Robbins, R. A.; Rana, R. R.; Loland, C. J.; Kobilka, B.; Stroud, R.; Byrne, B.; Gether, U.; Gellman, S. H. Tandem Facial Amphiphiles for Membrane Protein Stabilization. *J. Am. Chem. Soc.* **2010**, *132*, 16750−16752.
(10) Zhang, Q.; Ma, X.; Ward, A.; Hong, W.-X.; Jaakola, V.-P.; Stevens, R. C.; Finn, M. G.; Chang, G. Designing Facial Amphiphiles for the Stabilization of Integral Membrane Proteins. *Angew. Chem., Int. Ed.* **2007**, *46* (37), 7023−7025.
(11) Dauvergne, J.; Desuzinges, E. M.; Faugier, C.; Igonet, S.; Soulie, M.; Grousson, E.; Cornut, D.; Bonnete, F.; Durand, G.; Dejean, E.; Jawhari, A. Glycosylated Amphiphilic Calixarene-Based Detergent for Functional Stabilization of Native Membrane Proteins. *ChemistrySelect* **2019**, *4* (19), 5535−5539.
(12) Dufourc, E. J. Bicelles and nanodiscs for biophysical chemistry. *Biochim. Biophys. Acta, Biomembr.* **2021**, *1863* (1), 183478.
(13) Dürr, U. H.; Soong, R.; Ramamoorthy, A. When detergent meets bilayer: birth and coming of age of lipid bicelles. *Prog. Nucl. Magn. Reson. Spectrosc.* **2013**, *69*, 1−22.
(14) Thoma, J.; Burmann, B. M. Fake It 'Till You Make It—The Pursuit of Suitable Membrane Mimetics for Membrane Protein Biophysics. *Int. J. Mol. Sci.* **2021**, *22* (1), 50.
(15) Ratkeviciute, G.; Cooper, B. F.; Knowles, T. J. Methods for the solubilisation of membrane proteins: the micelle-aneous world of membrane protein solubilisation. *Biochem. Soc. Trans.* **2021**, *49* (4), 1763−1777.
(16) Popot, J.-L. Amphipols, nanodiscs, and fluorinated surfactants: three nonconventional approaches to studying membrane proteins in aqueous solutions. *Annu. Rev. Biochem.* **2010**, *79*, 737−775.
(17) Knowles, T. J.; Finka, R.; Smith, C.; Lin, Y.-P.; Dafforn, T.; Overduin, M. Membrane Proteins Solubilized Intact in Lipid Containing Nanoparticles Bounded by Styrene Maleic Acid Copolymer. *J. Am. Chem. Soc.* **2009**, *131* (22), 7484−7485.
(18) Craig, A. F.; Clark, E. E.; Sahu, I. D.; Zhang, R.; Frantz, N. D.; Al-Abdul-Wahid, M. S.; Dabney-Smith, C.; Konkolewicz, D.; Lorigan, G. A. Tuning the size of styrene-maleic acid copolymer-lipid nanoparticles (SMALPs) using RAFT polymerization for biophysical studies. *Biochim. Biophys. Acta* **2016**, *1858* (11), 2931−2939.
(19) Jamshad, M.; Charlton, J.; Lin, Y.-P.; Routledge, S.; Bawa, Z.; Knowles, T.; Overduin, M.; Dekker, N.; Dafforn, T.; Bill, R.; Poyner, D.; Wheatley, M. G-protein coupled receptor solubilization and purification for biophysical analysis and functional studies, in the total absence of detergent. *Biosci. Rep.* **2015**, *35* (2), No. e00188.
(20) Postis, V.; Rawson, S.; Mitchell, J. K.; Lee, S. C.; Parslow, R. A.; Dafforn, T. R.; Baldwin, S. A.; Muench, S. P. The use of SMALPs as a novel membrane protein scaffold for structure study by negative stain electron microscopy. *Biochim. Biophys. Acta, Biomembr.* **2015**, *1848* (2), 496−501.
(21) Swainsbury, D. J. K.; Scheidelaar, S.; van Grondelle, R.; Killian, J. A.; Jones, M. R. Bacterial Reaction Centers Purified with Styrene Maleic Acid Copolymer Retain Native Membrane Functional Properties and Display Enhanced Stability. *Angew. Chem., Int. Ed.* **2014**, *53* (44), 11803−11807.
(22) Kojima, K.; Sudo, Y. Expression of microbial rhodopsins in Escherichia coli and their extraction and purification using styrene-maleic acid copolymers. *STAR Protoc.* **2022**, *3* (1), 101046.
(23) Tedesco, D.; Maj, M.; Malarczyk, P.; Cingolani, A.; Zaffagnini, M.; Wnorowski, A.; Czapiński, J.; Benelli, T.; Mazzoni, R.; Bartolini, M.; Jóźwiak, K. Application of the SMALP technology to the isolation of GPCRs from low-yielding cell lines. *Biochim. Biophys. Acta, Biomembr.* **2021**, *1863* (9), 183641.
(24) Korotych, O. I.; Nguyen, T. T.; Reagan, B. C.; Burch-Smith, T. M.; Bruce, B. D. Poly(styrene-co-maleic acid)-mediated isolation of supramolecular membrane protein complexes from plant thylakoids. *Biochim. Biophys. Acta, Bioenerg.* **2021**, *1862* (3), 148347.
(25) Ayub, H.; Clare, M.; Milic, I.; Chmel, N. P.; Böning, H.; Devitt, A.; Krey, T.; Bill, R. M.; Rothnie, A. J. CD81 extracted in SMALP nanodiscs comprises two distinct protein populations within a lipid environment enriched with negatively charged headgroups. *Biochim. Biophys. Acta, Biomembr.* **2020**, *1862* (11), 183419.
(26) Lee, S. C.; Knowles, T. J.; Postis, V. L. G.; Jamshad, M.; Parslow, R. A.; Lin, Y.-p.; Goldman, A.; Sridhar, P.; Overduin, M.; Muench, S. P.; Dafforn, T. R. A method for detergent-free isolation of membrane proteins in their local lipid environment. *Nat. Protoc.* **2016**, *11* (7), 1149−1162.
(27) Smith, A. A. A.; Autzen, H. E.; Laursen, T.; Wu, V.; Yen, M.; Hall, A.; Hansen, S. D.; Cheng, Y.; Xu, T. Controlling Styrene Maleic Acid Lipid Particles through RAFT. *Biomacromolecules* **2017**, *18* (11), 3706−3713.
(28) Hall, S. C. L.; Tognoloni, C.; Price, G. J.; Klumperman, B.; Edler, K. J.; Dafforn, T. R.; Arnold, T. Influence of Poly(styrene-co-maleic acid) Copolymer Structure on the Properties and Self-Assembly of SMALP Nanodiscs. *Biomacromolecules* **2018**, *19* (3), 761−772.
(29) Neville, G. M.; Morrison, K. A.; Shilliday, E. R.; Doutch, J.; Dalgliesh, R.; Price, G. J.; Edler, K. J. The effect of polymer end-group on the formation of styrene − maleic acid lipid particles (SMALPs). *Soft Matter* **2023**, *19* (44), 8507−8518.
(30) Farrelly, M. D.; Korneev, D.; Martin, L. L.; Thang, S. H. Tethering Efficiency of Reversible Addition-Fragmentation Chain Transfer-Synthesized Styrene Maleic Acid Polymers and Associated Styrene Maleic Acid Lipid Nanoparticles on Gold Surfaces. *ChemPlusChem* **2025**, *90* (7), No. e202500173.
(31) Janson, K.; Zierath, J.; Kyrilis, F. L.; Semchonok, D. A.; Hamdi, F.; Skalidis, I.; Kopf, A. H.; Das, M.; Kolar, C.; Rasche, M.; Vargas, C.; Keller, S.; Kastritis, P. L.; Meister, A. Solubilization of artificial mitochondrial membranes by amphiphilic copolymers of different charge. *Biochim. Biophys. Acta, Biomembr.* **2021**, *1863* (12), 183725.
(32) Kopf, A. H.; Lijding, O.; Elenbaas, B. O. W.; Koorengevel, M. C.; Dobruchowska, J. M.; van Walree, C. A.; Killian, J. A. Synthesis and Evaluation of a Library of Alternating Amphipathic Copolymers to Solubilize and Study Membrane Proteins. *Biomacromolecules* **2022**, *23* (3), 743−759.
(33) Oluwole, A. O.; Danielczak, B.; Meister, A.; Babalola, J. O.; Vargas, C.; Keller, S. Solubilization of Membrane Proteins into Functional Lipid-Bilayer Nanodiscs Using a Diisobutylene/Maleic Acid Copolymer. *Angew. Chem., Int. Ed.* **2017**, *56* (7), 1919−1924.
(34) Gulamhussein, A. A.; Uddin, R.; Tighe, B. J.; Poyner, D. R.; Rothnie, A. J. A comparison of SMA (styrene maleic acid) and DIBMA (di-isobutylene maleic acid) for membrane protein purification. *Biochim. Biophys. Acta, Biomembr.* **2020**, *1862* (7), 183281.
(35) Früh, V.; IJzerman, A. P.; Siegal, G. How to catch a membrane protein in action: a review of functional membrane protein immobilization strategies and their applications. *Chem. Rev.* **2011**, *111* (2), 640−656.
(36) Liu, W.; Samanta, S. K.; Smith, B. D.; Isaacs, L. Synthetic mimics of biotin/(strept)avidin. *Chem. Soc. Rev.* **2017**, *46* (9), 2391−2403.
(37) Le Droumaguet, B.; Nicolas, J. Recent advances in the design of bioconjugates from controlled/living radical polymerization. *Polym. Chem.* **2010**, *1* (5), 563−598.
(38) Wang, Y.; van Steenbergen, M. J.; Beztsinna, N.; Shi, Y.; Lammers, T.; van Nostrum, C. F.; Hennink, W. E. Biotin-decorated all-HPMA polymeric micelles for paclitaxel delivery. *J. Controlled Release* **2020**, *328*, 970−984.
(39) Hong, C.-Y.; Pan, C. Y. Direct Synthesis of Biotinylated Stimuli-Responsive Polymer and Diblock Copolymer by RAFT Polymerization Using Biotinylated Trithiocarbonate as RAFT Agent. *Macromolecules* **2006**, *39*, 3517−3524.
(40) Bathfield, M.; D'Agosto, F.; Spitz, R.; Charreyre, M.-T.; Delair, T. Versatile Precursors of Functional RAFT Agents. Application to the Synthesis of Bio-Related End-Functionalized Polymers. *J. Am. Chem. Soc.* **2006**, *128*, 2546−2547.
(41) Jia, Z.; Liu, J.; Boyer, C.; Davis, T. P.; Bulmus, V. Functional Disulfide-Stabilized Polymer-Protein Particles. *Biomacromolecules* **2009**, *10*, 3253−3258.

https://doi.org/10.1021/acsapm.5c02955
ACS Appl. Polym. Mater. XXXX, XXX, XXX−XXX

(42) Gody, G.; Boullanger, P.; Ladavière, C.; Charreyre, M. T.; Delair, T. Biotin α-End-Functionalized Gradient Glycopolymers Synthesized by RAFT Copolymerization. *Macromol. Rapid Commun.* **2008**, *29* (6), 511−519.
(43) Basit, H.; Shivaji Sharma, K.; Van der Heyden, A.; Gondran, C.; Breyton, C.; Dumy, P.; Winnik, F. M.; Labbé, P. Amphipol mediated surface immobilization of FhuA: a platform for label-free detection of the bacteriophage protein pb5. *Chem. Commun.* **2012**, *48* (48), 6037−6039.
(44) Bosco, M.; Damian, M.; Chauhan, V.; Roche, M.; Guillet, P.; Fehrentz, J.-A.; Bonneté, F.; Polidori, A.; Banères, J.-L.; Durand, G. Biotinylated non-ionic amphipols for GPCR ligands screening. *Methods* **2020**, *180*, 69−78.
(45) Charvolin, D.; Perez, J.-B.; Rouvière, F.; Giusti, F.; Bazzacco, P.; Abdine, A.; Rappaport, F.; Martinez, K. L.; Popot, J.-L. The use of amphipols as universal molecular adapters to immobilize membrane proteins onto solid supports. *Proc. Natl. Acad. Sci. U.S.A.* **2009**, *106* (2), 405−410.
(46) Zalipsky, S. Functionalized Poly(ethylene glycols) for Preparation of Biologically Relevant Conjugates. *Bioconjugate Chem.* **1995**, *6* (2), 150−165.
(47) Knop, K.; Hoogenboom, R.; Fischer, D.; Schubert, U. S. Poly(ethylene glycol) in drug delivery: pros and cons as well as potential alternatives. *Angew. Chem., Int. Ed.* **2010**, *49* (36), 6288−6308.
(48) Grethen, A.; Oluwole, A. O.; Danielczak, B.; Vargas, C.; Keller, S. Thermodynamics of nanodisc formation mediated by styrene/maleic acid (2:1) copolymer. *Sci. Rep.* **2017**, *7* (1), 11517.
(49) Lin, S.; Das, A.; Theato, P. CO2-Responsive graft copolymers: synthesis and characterization. *Polym. Chem.* **2017**, *8* (7), 1206−1216.
(50) Cunningham, R. D.; Kopf, A. H.; Elenbaas, B. O. W.; Staal, B. B. P.; Pfukwa, R.; Killian, J. A.; Klumperman, B. Iterative RAFT-Mediated Copolymerization of Styrene and Maleic Anhydride toward Sequence- and Length-Controlled Copolymers and Their Applications for Solubilizing Lipid Membranes. *Biomacromolecules* **2020**, *21* (8), 3287−3300.
(51) Glueck, D.; Grethen, A.; Das, M.; Mmeka, O. P.; Patallo, E. P.; Meister, A.; Rajender, R.; Kins, S.; Räschle, M.; Victor, J.; Chu, C.; Etzkorn, M.; Köck, Z.; Bernhard, F.; Babalola, J. O.; Vargas, C.; Keller, S. Electroneutral Polymer Nanodiscs Enable Interference-Free Probing of Membrane Proteins in a Lipid-Bilayer Environment. *Small* **2022**, *18* (47), 2202492.
(52) Damian, M.; Marie, J.; Leyris, J. P.; Fehrentz, J. A.; Verdié, P.; Martinez, J.; Banères, J. L.; Mary, S. High constitutive activity is an intrinsic feature of ghrelin receptor protein: a study with a functional monomeric GHS-R1a receptor reconstituted in lipid discs. *J. Biol. Chem.* **2012**, *287* (6), 3630−3641.
(53) Damian, M.; Louet, M.; Gomes, A. A. S.; M'Kadmi, C.; Denoyelle, S.; Cantel, S.; Mary, S.; Bisch, P. M.; Fehrentz, J.-A.; Catoire, L. J.; Floquet, N.; Banères, J. L. Allosteric modulation of ghrelin receptor signaling by lipids. *Nat. Commun.* **2021**, *12* (1), 3938.
(54) Barrile, F.; M'Kadmi, C.; De Francesco, P. N.; Cabral, A.; García Romero, G.; Mustafá, E. R.; Cantel, S.; Damian, M.; Mary, S.; Denoyelle, S.; Banères, J. L.; Marie, J.; Raingo, J.; Fehrentz, J. A.; Perelló, M. Development of a novel fluorescent ligand of growth hormone secretagogue receptor based on the N-Terminal Leap2 region. *Mol. Cell. Endocrinol.* **2019**, *498*, 110573.
(55) Ballesteros, J. A.; Weinstein, H. [19] Integrated methods for the construction of three-dimensional models and computational probing of structure-function relations in G protein-coupled receptors. *Methods Neurosci.* **1995**, *25*, 366−428.
(56) Stroud, Z.; Hall, S. C. L.; Dafforn, T. R. Purification of membrane proteins free from conventional detergents: SMA, new polymers, new opportunities and new insights. *Methods* **2018**, *147*, 106−117.
(57) Dörr, J. M.; Scheidelaar, S.; Koorengevel, M. C.; Dominguez, J. J.; Schäfer, M.; van Walree, C. A.; Killian, J. A. The styrene−maleic acid copolymer: a versatile tool in membrane research. *Eur. Biophys. J.* **2016**, *45* (1), 3−21.
(58) Monjal, V.; Guillet, P.; Moreno, A.; Soulié, M.; Durand, G. Photo-induced polymerization of styrene-maleic acid copolymers for the extraction of membrane proteins. *J. Polym. Sci.* **2024**, *62* (23), 5277−5288.
(59) Rouault, A. A. J.; Srinivasan, D. K.; Yin, T. C.; Lee, A. A.; Sebag, J. A. Melanocortin Receptor Accessory Proteins (MRAPs): Functions in the melanocortin system and beyond. *Biochim. Biophys. Acta, Mol. Basis Dis.* **2017**, *1863*, 2462−2467.
(60) Cornejo, M. P.; Mustafá, E. R.; Cassano, D.; Banères, J. L.; Raingo, J.; Perello, M. The ups and downs of growth hormone secretagogue receptor signaling. *FEBS J.* **2021**, *288* (24), 7213−7229.
(61) Weis, W. I.; Kobilka, B. K. The Molecular Basis of G Protein-Coupled Receptor Activation. *Annu. Rev. Biochem.* **2018**, *87*, 897−919.
(62) Ferrandez, Y.; Dezi, M.; Bosco, M.; Urvoas, A.; Valerio-Lepiniec, M.; Le Bon, C.; Giusti, F.; Broutin, I.; Durand, G.; Polidori, A.; Popot, J.-L.; Picard, M.; Minard, P. Amphipol-Mediated Screening of Molecular Orthoses Specific for Membrane Protein Targets. *J. Membr. Biol.* **2014**, *247* (9−10), 925−940.
(63) Lindhoud, S.; Carvalho, V.; Pronk, J. W.; Aubin-Tam, M. E. SMA-SH: Modified Styrene-Maleic Acid Copolymer for Functionalization of Lipid Nanodiscs. *Biomacromolecules* **2016**, *17* (4), 1516−1522.

https://doi.org/10.1021/acsapm.5c02955
ACS Appl. Polym. Mater. XXXX, XXX, XXX−XXX